Forschungszentrum Jülich
in der Helmholtz-Gemeinschaft

Institut für Plasmaphysik
EURATOM Association, Trilateral Euregio Cluster

Modelling of Rotating Plasma States and their Stability Accounting for Neutral Beam Injection and Helical Perturbations

Cuma Yarim, Umur Daybelge, Albert Nicolai

Jül-4091

Modelling of Rotating Plasma States and their Stability Accounting for Neutral Beam Injection and Helical Perturbations

Cuma Yarim, Umur Daybelge, Albert Nicolai

Berichte des Forschungszentrums Jülich ; 4091
ISSN 0944-2952
Institut für Plasmaphysik
EURATOM Association, Trilateral Euregio Cluster Jül-4091

Zu beziehen durch: Forschungszentrum Jülich GmbH · Zentralbibliothek
D-52425 Jülich · Bundesrepublik Deutschland
☎ 02461 61-5220 · Telefax: 02461 61-6103 · e-mail: zb-publikation@fz-juelich.de

CONTENTS

Abstract

The revisited neoclassical transport theory for a collisional edge layer with steep radial gradients in the toroidal damping time scale is extended, to include the faster poloidal damping time scale. The evolution of the toroidal and poloidal rotation speeds is determined within the frame of neoclassical theory by two equations accounting for ambipolarity and momentum conservation. The timescales τ_T and τ_P for the evolution of toroidal, U_T, and poloidal, U_P, velocities are quite different and allow for an expansion with respect to τ_P/τ_T. The truncation of the expansion at the linear term, i.e., $U_T=U_{T0}+U_{T1}$, and $U_P= U_{P0}+ U_{P1}$, yields four equations for $U_{T0,1}$ and $U_{P0,1}$: A diffusion equation for U_{T0}, an ordinary differential equation for $U_{P0,1}$ depending on the U_{T0}-profile, an evolution equation for U_{T1} depending on the U_{P0}-profile are obtained by separating the secular parts from the fast varying parts. Resorting to TEXTOR-data and assuming in a first step a stationary profile for U_{T0} the time evolution of U_{P0} is computed, in particular it is shown that the U_{P0} is, in general, close to its neoclassical value, but has the characteristic deviations at the boundary as demanded by the revisited neoclassical theory . In order to determine the stability behavior of poloidal and toroidal rotations in a tokamak plasma, the dependence of the poloidal velocity on time and initial velocity is analysed. It is observed, that the poloidal and toroidal spin-up tendencies are strongly coupled by nonlocal interactions, although these evolve essentially on different time scales. Rotation speeds are also influenced by charge exchange interactions, neutral beam injection, or a radial polarization current.

1. Introduction

As experiments indicate, transition to the tokamak H-mode from the L-mode, which is connected to a drastic change in confinement characteristics, has a causal relationship to the sudden onset of a toroidal and/or poloidal rotation, and the rise of a radial electric field. Both type of rotations, although driven and damped by different mechanisms are somehow interrelated and serve to suppress instabilities in the edge dus to the velocity shear. Among the mechanisms which seem to trigger the spin-up tendencies of the plasma particle, momentum and energy sources are considered at the outer and inner parts of the plasma magnetic surfaces [1-3]. To trigger the toroidal rotation, contrary to expectations, an external momentum input as evoked, for example, by neutral beam injection is not necessary, as transition to H-mode can also be achieved by ion cyclotron radio frequency (ICRF) wave heating. Other observations indicate that the evolution of plasma rotation velocities is also related to the rise of transport barriers both in the main body and in the edge layer of tokamak plasma.

Various features of the experimental results obtained in, for example, Alcator C-Mod or JET - discharges, can be explained by both neoclassical [4] and anomalous [5] transport theories of the toroidal velocity which are, however, based on diverging assumptions about the collisionality of the edge layer. Both types of theories indicate that the toroidal rotation velocity in the center of the plasma column is determined by the gradient of the edge temperature pedestal and the momentum input, such as NBI. Steep radial gradients of density and temperature at transport barriers in collisional plasma edge layers were considered recently in the revisited neoclassical transport theory [6-8]. Included in the new theory are also the Mikhailowskii-Tsypin corrections [9] to the Braginskii's stress tensors. According to the accretion theory [5], a source of the angular momentum is at the plasma edge, and the rotation is led inward by the ion temperature gradient modes (ITG); and the rise of a steep density gradient well inside the plasma column should reduce the central toroidal velocity, as this would suppress the ITG modes. Revisited neoclassical theory, on the other hand, claims that the plasma edge in experiments like stationary Alcator C-Mod (ELM)-free Ohmic discharges is sufficiently collisional, and the onset of spontaneous toroidal rotation of central plasma during the transition to H-Mod is due to the nonlocal influence of the poloidal rotation velocity, which is modified at the edge from its neoclassical value by large gradients and finite Larmor radius effects. Indeed, the plasma can be considered collisional when the collisionality parameter given by $\hat{\nu}_i = qR\nu_i / c_i$, where c_i is ion thermal velocity, q safety factor, R is the major radius, and ν_i is the ion collision frequency, is larger than 0.22 [4]. At the edge of Alcator C-Mod discharges it is estimated that $Z_{eff} \approx 2$ and $\hat{\nu}_i \approx 6.25$. Further, the revisited neoclassical theory shows that the observed reduction of the central rotation velocity when an internal transport barrier (ITB) is formed can also be explained by the outward main ion flow which is necessary to balance the impurity ion influx.

The purpose of the present study is to study the complicated relationship between the evolutions of the poloidal and toroidal velocities at and near the steep radial gradients of temperature and density in tokamak edge plasmas. A new modification is introduced into the revisited neoclassical equations in order to take into account the proper time scales of the poloidal and toroidal rotations.

2. Ambipolarity

To analyze poloidal or toroidal rotation related phenomena in the edge layer, we use modified fluid equations including mass and momentum sources as derived in the revisited neoclassical theory for collision dominated toroidal plasma with steep gradients near the edge. It has been shown in this theory that if the parameter $\Lambda_1 \equiv (\nu_i/\Omega_i)(q^2R^2/rL_\psi)$ is larger than 1/3, then the parallel momentum equation needs a modification [6-8]. (Ω_i is the ion Larmor frequency, q the safety factor, R the major radius and L_ψ the temperatue gradient length.) For example, in the Alcator C-Mod discharges one can estimate that at the edge $\Lambda_1 \approx 0.84$ [8]. The modified neoclassical ambipolarity equation for discharges with circular cross section is found as an evolution equation for the toroidal velocity U_φ

$$m_i N_i \frac{\partial U^{(1)}_{\varphi,i}}{\partial t} = \frac{\partial}{\partial r}\left[\eta_{2,i}\left(\frac{\partial U^{(1)}_{\varphi,i}}{\partial r} - \frac{0.107 q^2}{1+Q^2/S^2}\frac{\partial \ln T_i}{\partial r}\frac{B_\varphi}{B_\theta}U^{(2)}_{\theta,i}\right)\right] \\ + m_i N_i (\dot{m}_{\varphi,i} - \nu_{CX} U_{\varphi,i}) + J_r B_\theta \tag{1}$$

Where U_θ is the poloidal velocity $Q = [4B_\varphi U^{(2)}_{\theta,i} - 2.5(T_i/e_i)\partial \ln N_i^2 T_i/\partial r]B^{-1}$, $S = (2r\chi_{\|,i}N_i^{-1})/q^2R^2$. $\chi_{\|,i} = 3.9 P_i/m_i \nu_i$ is the parallel heat diffusion coefficient and J_r a possible radial polarization current. The classical perpendicular viscosity coefficient is given by $\eta_{2,i} = 1.2 N_i T_i \nu_i/\Omega_i^2$. Ω_i is the ion cyclotron frequency, B_θ the poloidal and B_ϕ the toroidal field.

The charge-exchange-collision frequency can be approximated by $\nu_{cx} \cong (1/3) < \sigma v > n_n$, where n_n is the neutral particle density, factor 1/3 gives the approximate fraction of charge exchange neutrals leaving the plasma, and the rate-coefficient is $<\sigma v> \cong 0.5\times10^{-13}$ m^{-3} s^{-1}. Neutral density profile can be taken as $n_n = N_n \exp[(L_\psi/L_n)\,\xi]$, where N_n is the neutral density at the separatrix and L_n its decay length.

To simulate a particular experiment by means of the revisited theory, representative temperature and density profiles must be assumed. This can be achieved, for computational simplicity, by using elementary analytical functions and normalizing them by the measured or estimated values of e.g. the temperature at some radial positions, such as the separatrix, the 'inflexion' point (defined as the point of vanishing curvature of the profile), or the plasma center. For example, the temperature profile can be taken as

$$T(r) = \frac{1}{2}T_c\left[1 - \tanh(a + \frac{r - r_s}{L_\psi})\right], \tag{2}$$

where

$$a = \tanh^{-1}\left(1 - 2\frac{T_s}{T_c}\right) \tag{3}$$

where L_ψ is a scale for the temperature gradient and T_c , T_s are values of temperature at the plasma cnetre and separatrix, respectively. For ELM-free Ohmic Alcator C-Mod discharges a more realistic profile, normalized by the temperature T_{inf} at the inflection point r_{inf} of the temperature profile, can be given as

$$T = T_{inf}\left\{1-\tanh\left(\frac{r-r_{inf}}{\Delta}\right)+\left(\frac{T_c}{T_{inf}}-2\right)\left(1-\left(\frac{r}{r_{inf}}\right)^2\right)^2\right\}. \tag{4}$$

2.1 Time derivative of poloidal velocity

In Refs. [6, 8], in the equation derived for poloidal velocity terms involving time derivative of the poloidal velocity were neglected because of replacing $U_{||}$ with $(B_\varphi / B)U_\varphi$. The equation

$$U_{||} = \underbrace{\underbrace{\frac{B_\theta}{B}}_{\sim\mu}\underbrace{U_\theta}_{\sim\mu^2 c_i}}_{\sim\mu^3 c_i} + \underbrace{\underbrace{\frac{B_\varphi}{B}}_{\sim 1}\underbrace{U_\varphi}_{\sim\mu c_i}}_{\sim\mu c_i}$$

means that terms of the order $\mu^3 c_i$ are neglected in Refs. [6, 8]. $\mu\sim0.1$, which was defined in the revisited neoclassical theory as the ratio $\mu\sim B_\theta/B_\varphi \sim L_\psi/r \sim r/qR$, where L_ψ is the scale length of radial gradients [6], is used here for order of magnitude estimates.

This approach is reasonable in studying such cases of longer time behaviour of the velocities. Thus, if the first term in the preceding equation is neglected, the time evolution of the poloidal velocity is synchronized with that of the toroidal velocity. It is known, however, that the toroidal and poloidal velocities have different damping times. In Ref. [10] poloidal and toroidal damping times were shown to be ordered as

$$\tau_P < O[\,(a_i/r)^2,(\nu_{cx}/\nu_i)\,]\tau_T \ll \tau_T \tag{5}$$

The contribution of the time derivative of the poloidal velocity to the JB weighted parallel momentum equation can be calculated as follows:

$$\begin{aligned}\oint JB\frac{d\theta}{2\pi}m_i N_i\frac{\partial U_{||}}{\partial t} &= \oint h_r h_\theta h_\varphi B\frac{d\theta}{2\pi}m_i N_i\left[\frac{B_\theta}{B}\frac{\partial U_\theta}{\partial t}+\frac{B_\varphi}{B}\frac{\partial U_\varphi}{\partial t}\right]\\ &= \oint\frac{d\theta}{2\pi}m_i N_i\left[r\frac{\partial U_\theta}{\partial t}+r\frac{B_\varphi}{B_\theta}\frac{\partial U_\varphi}{\partial t}\right] = m_i N_i^{(0)}\left[r\frac{\partial U_\theta^{(2)}}{\partial t}+qR\frac{\partial U_\varphi^{(1)}}{\partial t}\right]\end{aligned} \tag{6}$$

where, $\nabla\cdot\vec{B}=0 \Rightarrow h_r h_\varphi B_\theta = 1$ has been used. By adding this new term into the parallel momentum equation obtained by Ref. [8], one gets [10, 11] the Eq. (7). The Pfirsch-Schlüter factor for inertia enhancement on the left hand side of Eq. (7) depends on the collisionality and can be altered in the plateau regime [12]. The superscripts on rotation velocities in above equations reflect their respective orders in a small parameter. An outline of the derivation of the toroidal and parallel momentum equations in the revisited neoclassical theory can be found in Appendix A. Appendix B gives a rigorous derivation of the inertia enhancement factor in the parallel momentum equation.

$$
\begin{aligned}
m_i N_i (1+2q^2)\frac{\partial U^{(2)}_{\theta,i}}{\partial t} &= -\frac{3\eta_{0,i}}{2R^2}\left(U^{(2)}_{\theta,i} + 1.833(e_i B_\varphi)^{-1}\frac{\partial T_i}{\partial r}\right) \\
&+ 0.54\frac{\eta_{2,i}}{1+Q^2/S^2} q^2 \frac{e_i B_\varphi}{T_i}\frac{\partial \ln T_i}{\partial r}\left[\frac{T_i}{e_i B_\theta}\frac{\partial U^{(1)}_{\varphi,i}}{\partial r} + \frac{1}{2}U^{(1)2}_{\varphi,i}\right. \\
&\left. - U^{(1)}_{\varphi,i}\frac{B_\varphi}{B_\theta}\left(U^{(2)}_{\theta,i} - \frac{T_i}{e_i B_\varphi}\frac{\partial \ln N_i^2 T_i}{\partial r}\right) + 1.90\frac{B_\varphi^2}{B_\theta^2}\left(U^{(2)}_{\theta,i} - 0.8\frac{T_i}{e_i B_\varphi}\frac{\partial \ln N_i^{1.6} T_i}{\partial r}\right)^2\right] \\
&- J_r B_\varphi
\end{aligned}
\tag{7}
$$

2.2 Dimensionless equations

The toroidal and the poloidal velocities are taken as $U_{\varphi,i} = (B_{\theta\,sep}/B_\varphi)c_{i\,sep}\,\hat{x}$, $U_{\theta,i} = (B_{\theta\,sep}/B_\varphi)^2 c_{i\,sep}\,\hat{y}$, respectively. The radial coordinate r, the temperature, T_i, and the density, N_i, will be non-dimensionalized as follows; $r = r_{sep} + L_\psi\,\hat{\xi}$, $T_i = T_{sep}\,\hat{T}$, $N_i = N_{sep}\,\hat{N}$, $t = \tau_T\,\hat{t}$ where $\hat{x}$, $\hat{y}$, $\hat{\xi}$, $\hat{T}$, $\hat{N}$ and $\hat{t}$ denote the non-dimensionalized toroidal and poloidal velocities, radial coordinate, temperature, density and time, respectively. $c_{i\,sep}$, T_{sep}, and N_{sep} are the ion thermal velocity, temperature and density at the separatrix whose radial coordinate is r_{sep}. L_ψ is temperature gradient length scale at the separatrix, and τ_T is the toroidal time scale. Inserting these expressions in the toroidal momentum equation, one gets

$$
\begin{aligned}
& m_i N_{isep}\frac{B_{\theta sep}}{B_\varphi}\frac{c_{isep}}{\tau_T}\hat{N}\frac{\partial \hat{x}}{\partial \hat{t}} \\
&= \frac{B_{\theta sep}}{B_\varphi}\frac{\eta_{2sep} c_{isep}}{L_\psi^2}\frac{\partial}{\partial \hat{\xi}}\left[\hat{\eta}_2\left(\frac{\partial \hat{x}}{\partial \hat{\xi}} + \frac{0.107 q^2}{1+Q^2/S^2}\frac{B_{\theta sep}}{B_\varphi}\frac{\partial \ln T_i}{\partial \xi}\hat{y}\right)\right] \\
&\quad - \frac{m_i N_{isep} L_\psi^2}{\eta_{2sep}}\nu_{CX}\hat{N}\hat{x} + \frac{m_i N_{isep} L_\psi^2}{\eta_{2sep} c_{isep}}\frac{B_\varphi}{B_{\theta sep}}\hat{N}\dot{m}_{\varphi,i} + \frac{B_\varphi}{B_{\theta sep}}\frac{L_\psi^2}{\eta_{2sep} c_{isep}} J_r B_\varphi
\end{aligned}
\tag{8}
$$

Since all the terms in the above equation should have the same order, an estimate can be obtained for the toroidal time scale τ_T, by taking the ratio of the l.h.s of the equation (8) and the first term of the r.h.s. The dimensionless terms are considered to be of the order 1. Following the scaling relationships given by Ref. [6]:

$$
\frac{m_i N_{isep}}{\tau_T}\frac{L_\psi^2}{\eta_{2sep}} \sim \frac{\tau_{isep}}{\tau_T}\frac{L_\psi^2}{c_{isep}^2}\Omega_i^2 \sim \frac{\tau_{isep}}{\tau_T}\left(\frac{R\nu_{isep}}{c_{isep}}\frac{L_\psi}{r}\frac{r}{R}\frac{\Omega_i}{\nu_{isep}}\right)^2 \sim \frac{\tau_{isep}}{\tau_T}\mu^{-4} \sim 1
$$

is obtained and hence

$$
\tau_T \sim \mu^{-4}\,\tau_{isep} \equiv \mu^{-4}\,\nu_{isep}^{-1}\,. \tag{9}
$$

For the numerical values of the time scales see Appendix C.

The resulting dimensionless toroidal momentum equation is:

$$p_1 \frac{\partial \hat{x}}{\partial \hat{t}} = \frac{\partial}{\partial \hat{\xi}}\left[p_2 \frac{\partial \hat{x}}{\partial \hat{\xi}} + \frac{p_3\, \hat{y}}{1+p_4(\hat{y}+p_5)^2} \right] + p_6\, \hat{x} + p_7 \tag{10}$$

Where the the dimensionless quantities $p_{1\text{-}7}$ are given by

$$p_1 = \frac{m_i\, N_{sep}\, L_\psi^2}{\tau_T\, \eta_{2sep}} \hat{N} \tag{10a}$$

$$p_2 = \hat{\eta}_2 \tag{10b}$$

$$p_3 = -0.107\, q^2\, \hat{\eta}_2 \frac{B_{\theta sep}}{B_\theta} \frac{\partial \ln T_i}{\partial \hat{\xi}} \tag{10c}$$

$$p_4 = \left(0.51 \frac{B_{\theta sep}^2}{B_\theta^2} \frac{r_{sep}\, \nu_{isep}}{c_{isep}} \frac{r}{r_{sep}} \frac{\hat{\nu}_i}{\hat{T}} \right)^2 \tag{10d}$$

$$p_5 = -0.625\, M \hat{T} \frac{\partial \ln N_i^2\, T_i}{\partial \hat{\xi}} \tag{10e}$$

$$p_6 = -\frac{m_i\, N_{sep}\, L_\psi^2\, \nu_{cxsep}}{\eta_{2sep}} \hat{N} \exp\left(\frac{L_\psi}{L_{neu}} \hat{\xi} \right) \tag{10f}$$

$$p_7 = \frac{m_i\, N_{sep}\, L_\psi^2\, \dot{m}_{\varphi,isep}}{\eta_{2sep}\, c_{isep}} \frac{B_\varphi}{B_{\theta sep}} \hat{N} \left(\frac{r}{rsep} \right)^{-3/2} + \frac{L_\psi^2}{\eta_{2sep}\, c_{isep}} \frac{B_\varphi}{B_{\theta sep}} J_r\, B_\theta \tag{10g}$$

with

$$M = \frac{T_{sep}}{e_i\, B_\varphi\, L_\psi\, c_{isep}} \frac{B_\varphi^2}{B_{\theta sep}^2} \tag{10h}$$

Using the same procedure the parallel momentum equation can be written as follows:

$$\begin{aligned} &\frac{m_i\, N_{isep}\, c_{isep}}{\tau_T} \hat{N}(1+2q^2) \frac{B_{\theta sep}^2}{B_\varphi^2} \frac{\partial \hat{y}}{\partial \hat{t}} = \\ &-\frac{3}{2} \frac{\eta_{0,isep}\, c_{isep}}{R^2} \frac{B_{\theta sep}^2}{B_\varphi^2} \hat{\eta}_0 \left(\hat{y} + 1.833 \frac{T_{isep}}{e_i\, B_\varphi\, L_\psi\, c_{isep}} \frac{B_\varphi^2}{B_{\theta sep}^2} \hat{T} \frac{\partial \ln T_i}{\partial \hat{\xi}} \right) \\ &+0.54 \frac{\eta_{2,isep}\, q^2}{1+Q^2/S^2} \frac{e_i\, B_\varphi\, c_{isep}^2}{T_{isep}\, L_\psi} \frac{B_{\theta sep}^2}{B_\varphi^2} \frac{\hat{\eta}_2}{\hat{T}} \frac{\partial \ln T_i}{\partial \hat{\xi}} \left[\frac{B_{\theta sep}}{B_\theta} M \hat{T} \frac{\partial \hat{x}}{\partial \hat{\xi}} + \frac{1}{2} \hat{x}^2 \right. \\ &\left. - \frac{B_{\theta sep}}{B_\theta} \hat{x} \left(\hat{y} - M \hat{T} \frac{\partial \ln N_i^2\, T_i}{\partial \hat{\xi}} \right) + 1.90 \frac{B_{\theta sep}^2}{B_\theta^2} \left(\hat{y} - 0.8 M \hat{T} \frac{\partial \ln N_i^{1.6}\, T_i}{\partial \hat{\xi}} \right)^2 \right] - J_r\, B_\varphi \end{aligned} \tag{11}$$

The ratio of the l.h.s of the above equation and the first term of the r.h.s is

$$\frac{\dfrac{m_i\, N_{isep}\, c_{isep}}{\tau_T}\dfrac{B^2_{\theta sep}}{B^2_\varphi}}{-\dfrac{3}{2}\dfrac{\eta_{0,isep}\, c_{isep}}{R^2}\dfrac{B^2_{\theta sep}}{B^2_\varphi}} \sim \frac{m_i\, N_{isep}\, R^2}{\tau_T}\frac{1}{0.96\, N_{isep}\, T_{isep}\, \tau_{isep}} \sim \left(\frac{R\, \nu_{isep}}{c_{isep}}\right)^2 \frac{\tau_{isep}}{\tau_T} \sim \mu^2$$

Or, as expected, the ratio of the l.h.s and the second term of the r.h.s is of the same order:

$$\frac{\dfrac{m_i\, N_{isep}\, c_{isep}}{\tau_T}\dfrac{B^2_{\theta sep}}{B^2_\varphi}}{0.54\,\eta_{2,isep}\dfrac{e_i\, B_\varphi c^2_{isep}}{L_\psi\, T_{isep}}\dfrac{B^2_{\theta sep}}{B^2_\varphi}} \sim \frac{m_i\, N_{isep}\, L_\psi\, T_{isep}}{e_i\, B_\varphi\, c_{isep}\, \tau_T}\frac{\Omega_{isep}\, \tau_{isep}}{1.2\, N_{isep}\, T_{isep}} \sim \frac{\tau_{isep}}{\tau_T}\frac{L_\psi}{a_{isep}} \sim \mu^2$$

So, the factor $B^2_{\theta sep}/B^2_\varphi$ stays on the l.h.s. of the equation (11), thus:

$$\begin{aligned} &\varepsilon\frac{\partial\hat{y}}{\partial t} = q_1(\hat{y}+q_2) \\ &\qquad + \frac{q_3}{1+p_4(\hat{y}+p_5)^2}\left[q_4\frac{\partial\hat{x}}{\partial\hat{\xi}} + \frac{1}{2}\hat{x}^2 + q_5\,\hat{x}(\hat{y}+q_6) + q_7(\hat{y}+q_8)^2\right] + q_9 \end{aligned} \tag{12}$$

Where the following definitions were used:

$$\varepsilon = \frac{B^2_{\theta sep}}{B^2_\varphi} \sim \mu^2 \tag{12a}$$

$$q_1 = -\frac{3}{2}\frac{1}{(1+2q^2)}\frac{\eta_{0,isep}}{R^2}\frac{\tau_T}{m_i\, N_{sep}}\frac{B^2_{\theta sep}}{B^2_\varphi}\frac{\hat{\eta}_0}{\hat{N}} \tag{12b}$$

$$q_2 = 1.833\, M\hat{T}\frac{\partial \ln T_i}{\partial\hat{\xi}} \tag{12c}$$

$$q_3 = 0.54\frac{1}{(1+2q^2)}\frac{e_i\, B_\varphi\, c_{isep}}{T_{sep}\, L_\psi}\frac{\eta_{2sep}\, \tau_T\, q^2}{m_i\, N_{sep}}\frac{B^2_{\theta sep}}{B_\varphi}\frac{\hat{\eta}_2}{\hat{N}\hat{T}}\frac{\partial \ln T_i}{\partial\hat{\xi}} \tag{12d}$$

$$q_4 = \frac{B_{\theta sep}}{B_\theta} M\hat{T} \tag{12e}$$

$$q_5 = -\frac{B_{\theta sep}}{B_\theta} \tag{12f}$$

$$q_6 = -M\hat{T}\frac{\partial \ln N_i^2\, T_i}{\partial\hat{\xi}} \tag{12g}$$

$$q_7 = 1.90\frac{B^2_{\theta sep}}{B^2_\theta} \tag{12h}$$

$$q_8 = -\,0.8\, M\hat{T}\frac{\partial \ln N_i^{1.6}\, T_i}{\partial\hat{\xi}} \tag{12i}$$

$$q_9 = -\frac{1}{(1+2q^2)}\frac{\tau_T}{m_i\, N_{isep}\, c_{isep}}\frac{J_r\, B_\varphi}{\hat{N}} \tag{12j}$$

2.3 Multiple-time-scale analysis

By omitting hat sign for the non-dimensional variables and defining a new faster time scale by $\tau \equiv t/\varepsilon$ we obtain the following set of equations:

$$p_1 \frac{\partial x}{\partial \tau} = \varepsilon \left\{ \frac{\partial}{\partial \xi}\left[p_2 \frac{\partial x}{\partial \xi} + \frac{p_3\, y}{1+p_4 (y+p_5)^2} \right] + p_6\, x + p_7 \right\} \tag{13a}$$

$$\frac{\partial y}{\partial \tau} = q_1 (y+q_2) + \frac{q_3}{1+p_4(y+p_5)^2}\left[q_4 \frac{\partial x}{\partial \xi} + \frac{1}{2}x^2 + q_5\, x(y+q_6) + q_7 (y+q_8)^2 \right] + q_9 \tag{13b}$$

The importance of the second time scale, for example, for high frequency or transient behaviour of both spin-up phenomena becomes obvious.

Now we have two time scale: a) The slow time scale: $\tau_T \sim \mu^{-4}\, \tau_{isep}$; and b) the fast time scale: $\tau_P \sim \varepsilon\, \tau_T \sim \mu^{-2}\, \tau_{isep}$. We apply a multiple time-scale analysis to the above set of equations [13]. The evolution of the poloidal and the toroidal velocities will depend not only on the slow time scale, t, and the radial coordinate, ξ, but also on the fast time scale, τ.

Since ε can be considered as small, we use the expansion

$$x = x(t,\tau,\xi) = x_0(t,\tau,\xi) + \varepsilon\, x_1(t,\tau,\xi) \tag{14a}$$

$$y = y(t,\tau,\xi) = y_0(t,\tau,\xi) + \varepsilon\, y_1(t,\tau,\xi) \tag{14b}$$

where the subscript (1) stands for the fast and the subscript (0) the slow time scale..

Since τ can be understood as a function of t, we replace the fast time derivative by:

$$\frac{\partial}{\partial \tau} \to \frac{\partial}{\partial \tau} + \frac{\partial}{\partial t}\frac{\partial t}{\partial \tau} = \frac{\partial}{\partial \tau} + \varepsilon \frac{\partial}{\partial t}$$

Substituting these expressions into the time derivatives of the velocities, we get:

$$\frac{\partial x}{\partial \tau} \to \left(\frac{\partial}{\partial \tau} + \varepsilon \frac{\partial}{\partial t} \right)(x_0 + \varepsilon\, x_1) = \frac{\partial x_0}{\partial \tau} + \varepsilon \left(\frac{\partial x_0}{\partial t} + \frac{\partial x_1}{\partial \tau} \right)$$

$$\frac{\partial y}{\partial \tau} \to \left(\frac{\partial}{\partial \tau} + \varepsilon \frac{\partial}{\partial t} \right)(y_0 + \varepsilon\, y_1) = \frac{\partial y_0}{\partial \tau} + \varepsilon \left(\frac{\partial y_0}{\partial t} + \frac{\partial y_1}{\partial \tau} \right)$$

Noticing the following relationships:

$$(K+\varepsilon L)^2 \approx K^2 + \varepsilon(2KL) \tag{15a}$$

$$\frac{1}{K+\varepsilon L} = \frac{1}{K}\frac{1}{1+\varepsilon L/K} \approx \frac{1}{K} - \varepsilon \frac{L}{K^2} \tag{15b}$$

$$(K+\varepsilon L)(M+\varepsilon N)\approx KM+\varepsilon(KN+LM) \tag{15c}$$

we get the following expressions for some coefficients of the equations (13a) and (13b).

$$\frac{1}{1+p_4(y+p_5)^2}\approx A+\varepsilon B, \tag{16a}$$

$$\frac{y}{1+p_4(y+p_5)^2}\approx D+\varepsilon E \tag{16b}$$

Where A, B, C and E are given by

$$A=\frac{1}{1+p_4(y_0+p_5)^2}, \tag{17a}$$

$$B=\frac{-2p_4\,y_1(y_0+p_5)}{[1+p_4(y_0+p_5)^2]^2}, \tag{17b}$$

$$D=\frac{y_0}{1+p_4(y_0+p_5)^2}, \tag{17c}$$

and

$$E=\left\{\frac{y_1}{1+p_4(y_0+p_5)^2}-\frac{2p_4\,y_0\,y_1(y_0+p_5)}{[1+p_4(y_0+p_5)^2]^2}\right\} \tag{17d}$$

Substituting all these expressions in the equations (13a) and (13b), we get for the toroidal momentum equation

$$p_1\frac{\partial x_0}{\partial \tau}+\varepsilon p_1\left(\frac{\partial x_0}{\partial t}+\frac{\partial x_1}{\partial \tau}\right)\approx\varepsilon\left\{\frac{\partial}{\partial \xi}\left[p_2\frac{\partial x_0}{\partial \xi}+p_3 D\right]+p_6 x_0+p_7\right\} \tag{18a}$$

and for the parallel momentum equation

$$\begin{aligned}\frac{\partial y_0}{\partial \tau}+\varepsilon\left(\frac{\partial y_0}{\partial t}+\frac{\partial y_1}{\partial \tau}\right)&\approx q_1(y_0+q_2)\\ &+q_3 A\left[q_4\frac{\partial x_0}{\partial \xi}+\frac{1}{2}x_0^2+q_5 x_0(y_0+q_6)+q_7(y_0+q_8)^2\right]+q_9\\ &+\varepsilon\left\{q_1 y_1+q_3 B\left[q_4\frac{\partial x_0}{\partial \xi}+\frac{1}{2}x_0^2+q_5 x_0(y_0+q_6)+q_7(y_0+q_8)^2\right]\right.\\ &\left.+q_4 A\left[q_4\frac{\partial x_1}{\partial \xi}+x_0 x_1+q_5 x_0 y_1+q_5 x_1(y_0+q_6)+2q_7 y_1(y_0+q_8)^2\right]\right\}\end{aligned} \tag{18b}$$

Comparing the coefficients of ε and the ε-independent terms, we obtain 4 equations for the 4 unknowns (x_0, x_1, y_0, y_1):

$$\frac{\partial x_0}{\partial \tau}=0 \tag{19a}$$

$$p_1 \frac{\partial x_1}{\partial \tau} + p_1 \frac{\partial x_0}{\partial t} = \frac{\partial}{\partial \xi}\left[p_2 \frac{\partial x_0}{\partial \xi} + p_3 D \right] + p_6 x_0 + p_7 \tag{19b}$$

$$\frac{\partial y_0}{\partial \tau} = q_1 (y_0 + q_2) + q_3 A \left[q_4 \frac{\partial x_0}{\partial \xi} + \frac{1}{2} x_0^2 + q_5 x_0 (y_0 + q_6) + q_7 (y_0 + q_8)^2 \right] + q_9 \tag{19c}$$

$$\begin{aligned} \frac{\partial y_0}{\partial t} + \frac{\partial y_1}{\partial \tau} &= q_1 y_1 + q_3 B \left[q_4 \frac{\partial x_0}{\partial \xi} + \frac{1}{2} x_0^2 + q_5 x_0 (y_0 + q_6) + q_7 (y_0 + q_8)^2 \right] \\ &+ q_4 A \left[q_4 \frac{\partial x_1}{\partial \xi} + x_0 x_1 + q_5 x_0 y_1 + q_5 x_1 (y_0 + q_6) + 2 q_7 y_1 (y_0 + q_8)^2 \right] \end{aligned} \tag{19d}$$

The equation (19a) implies that the toroidal velocity is constant at the fast time scale, in other words the toroidal velocity can depend only on ξ, and the slow time t.

Therefore equation (19b) has terms which depend on t and ξ only, as can be seen by rewriting equation (19b)

$$\begin{aligned} p_1 \frac{\partial x_1 (t,\tau,\xi)}{\partial \tau} + p_1 \frac{\partial x_0 (t,\xi)}{\partial t} &= \frac{\partial}{\partial \xi}\left[p_2 \frac{\partial x_0 (t,\xi)}{\partial \xi} \right] + p_6 x_0 (t,\xi) + p_7 \\ &+ \frac{\partial}{\partial \xi}\left[\frac{p_3 y_0 (t,\tau,\xi)}{1 + p_4 \left(y_0 (t,\tau,\xi) + p_5 \right)^2} \right] \end{aligned} \tag{19b'}$$

A solution for $x_1 (t,\tau,\xi)$ can be found, only if

$$p_1 \frac{\partial x_0 (t,\xi)}{\partial t} = \frac{\partial}{\partial \xi}\left[p_2 \frac{\partial x_0 (t,\xi)}{\partial \xi} \right] + p_6 x_0 (t,\xi) + p_7 \tag{19b''}$$

holds [13].

2.4 Integration of the poloidal velocity on the fast time scale

The third equation of this set, equation (19c), can be integrated along fast time scale, τ, since x_0 does not depend on τ. During the integration x_0, and $\partial x_0 / \partial \xi$ can be considered as constant parameters. This equation may be written as follows,

$$d\tau = \frac{g_2 (y_0)}{f_3 (y_0)} d y_0 = \frac{\kappa y_0^2 + \lambda y_0 + \mu}{y_0^3 + \beta y_0^2 + \gamma y_0 + \delta} d y_0 \tag{20}$$

where

$$\kappa = \frac{1}{q_1} \tag{20a}$$

$$\lambda = \frac{2 p_5}{q_1} \tag{20b}$$

$$\mu = \frac{1 + p_4 p_5^2}{q_1 p_4} \tag{20c}$$

$$\beta=\frac{2q_1 p_4 p_5+p_4(q_1 q_2+q_9)+q_{12}}{q_1 p_4} \tag{20d}$$

$$\gamma=\frac{q_1(1+p_4 p_5^2)+2p_4 p_5(q_1 q_2+q_9)+2q_8 q_{12}+q_{11}}{q_1 p_4} \tag{20e}$$

$$\delta=\frac{(q_1 q_2+q_9)(1+p_4 p_5^2)+q_{11} q_6+q_{12} q_8^2+q_{10}}{q_1 p_4} \tag{20f}$$

and

$$q_{10}=q_3\left(q_4\frac{\partial x_0}{\partial \xi}+\frac{1}{2}x_0^2\right) \tag{20g}$$

$$q_{11}=q_3 q_5 x_0 \tag{20h}$$

$$q_{12}=q_3 q_7 \tag{20i}$$

One real root is always guaranteed for the cubic polynomial at the denominator of the l.h.s. of equation (20). Let this root be 'a'. For the prescribed coefficients (calculated at one radial coordinate), this root can be found numerically, for example, by bisection method. Then the cubic polynomial can be expressed as two factor:

$$f_3(y_0)=y_0^3+\beta y_0^2+\gamma y_0+\delta=(y_0-a)[y_0^2+(\beta+a)y_0+\gamma+a(\beta+a)]$$

For the other two roots, the discriminant, Δ, is:

$$\Delta=(\beta+a)^2-4[\gamma+a(\beta+a)] \tag{21}$$

There are two cases:

i) If $\Delta\geq 0$; the roots of the cubic polynomial becomes: a, b, c (three real roots)

$$\int_0^\tau d\tau=\int_{y_0(0)}^{y_0}\frac{\kappa y_0^2+\lambda y_0+\mu}{y_0^3+\beta y_0^2+\gamma y_0+\delta}dy_0=\int_{y_0(0)}^{y_0}\left[\frac{A}{y_0-a}+\frac{B}{y_0-b}+\frac{C}{y_0-c}\right]dy_0$$

and the result of the integration is:

$$\tau=A\ln\left|\frac{y_0-a}{y_0(0)-a}\right|+B\ln\left|\frac{y_0-b}{y_0(0)-b}\right|+C\ln\left|\frac{y_0-c}{y_0(0)-c}\right| \tag{22}$$

where

$$A=\frac{g_2(a)}{f_3'(a)}; \tag{22a}$$

$$B=\frac{g_2(b)}{f_3'(b)}; \tag{22b}$$

$$C=\frac{g_2(c)}{f_3'(c)} \tag{22c}$$

here prime denotes the derivative with respect to the argument.

ii) If $\Delta<0$; the roots of the cubic polynomial becomes: $a, b_{re}+i\,b_{im}, b_{re}-i\,b_{im}$ (one real, two complex roots)

$$b_{re}=-\frac{\beta+a}{2}; \tag{22d}$$

$$b_{im}=\sqrt{\gamma+a(\beta+a)-\frac{(\beta+a)^2}{4}} \tag{22e}$$

$$\begin{aligned}\int_0^{\tau} d\tau &= \int_{y_0(0)}^{y_0} \frac{\kappa y_0^2+\lambda y_0+\mu}{y_0^3+\beta y_0^2+\gamma y_0+\delta} d y_0 \\ &= \int_{y_0(0)}^{y_0} \left[\frac{A}{y_0-a}+\frac{B_{re}+i\,B_{im}}{y_0-b_{re}-i\,b_{im}}+\frac{B_{re}-i\,B_{im}}{y_0-b_{re}+i\,b_{im}}\right] d y_0\end{aligned}$$

and the integration yields:

$$\begin{aligned}\tau = {} & A \ln\left|\frac{y_0-a}{y_0(0)-a}\right| + B_{re} \ln\left|\frac{(y_0-b_{re})^2+b_{im}^2}{[y_0(0)-b_{re}]^2+b_{im}^2}\right| \\ & -2B_{im}\left[\tan^{-1}\left(\frac{y_0-b_{re}}{b_{im}}\right)-\tan^{-1}\left(\frac{y_0(0)-b_{re}}{b_{im}}\right)\right]\end{aligned} \tag{23}$$

where

$$A=\frac{g_2(a)}{f_3'(a)}; \tag{23a}$$

$$B_{re}=\text{Real}\left[\frac{g_2(b_{re}+i\,b_{im})}{f_3'(b_{re}+i\,b_{im})}\right]; \tag{23b}$$

$$B_{im}=\text{Imaginary}\left[\frac{g_2(b_{re}+i\,b_{im})}{f_3'(b_{re}+i\,b_{im})}\right]; \tag{23c}$$

$$B_{re}=\frac{B_{nr}B_{dr}+B_{ni}B_{di}}{B_{dr}^2+B_{di}^2}; \tag{23b'}$$

$$B_{im}=\frac{B_{ni}B_{dr}-B_{nr}B_{di}}{B_{dr}^2+B_{di}^2} \tag{23c'}$$

with

$$B_{nr}=\kappa(b_{re}^2-b_{im}^2)+\lambda b_{re}+\mu, \tag{23d}$$

$$B_{ni}=b_{im}(2\kappa b_{re}+\lambda) \tag{23e}$$

$$B_{dr}=3(b_{re}^2-b_{im}^2)+2\beta b_{re}+\gamma, \tag{23f}$$

$$B_{ni}=2b_{im}(3b_{re}+\beta) \tag{23g}$$

3. Stability Analysis and Results of a Parametrical Study

Now, we can summarize the behaviour of y_0 for increasing τ by means of coefficients A, B, and C, as follows:

1) Case of f_3 having three real zeros:

a) if $A+B+C < 0$, then for all initial values y_0 remains stable.

b) if $A+B+C \geq 0$, then some initial values will choose an unstable branch, and y_0 will move along this unstable branch. To decide about the stability of a chosen branch, one must either look at the branching map, or use a logical classification based on the critical points of the branches, as follows: Supposing that the zeros of f_3 are ordered as $a<b<c$, then y_0 is always stable for $a < y_0(0) < c$. If, however, $c < y_0(0)$, or $y_0(0) < a$, then one must also look at the zeros of g_2, i.e., s_1 and s_2. Supposing these are ordered as

$s_1 < s_2$, then if

i) $(c, s_2) < y_0(0)$, then y_0 is unstable;

ii) $c < y_0(0) < s_2$, then y_0 is stable;

iii) $y_0(0) < (a, s_1)$, then y_0 is unstable;

iv) $s_1 < y_0(0) < a$, then y_0 is stable.

2) Case of f_3 having only one real zero:

a) if $A+2B_{re}<0$, then for all initial values, y_0 moves on some stable branches.

b) if $A+2B_{re}\geq 0$, then stability of y_0 depends on the chosen initial value. In this case we can again determine stability using an analogous scheme as in case 1-b).

Two exemplary branching maps are seen in Figures 3.1 and 3.2. In the Figure 3.1, case of three real zeros have been represented. Here, there are some initial conditions after which the time is not increasing, which is thought to be corrected by calculating the higher approximation. Figure 3.2 represents the case of one real zero.

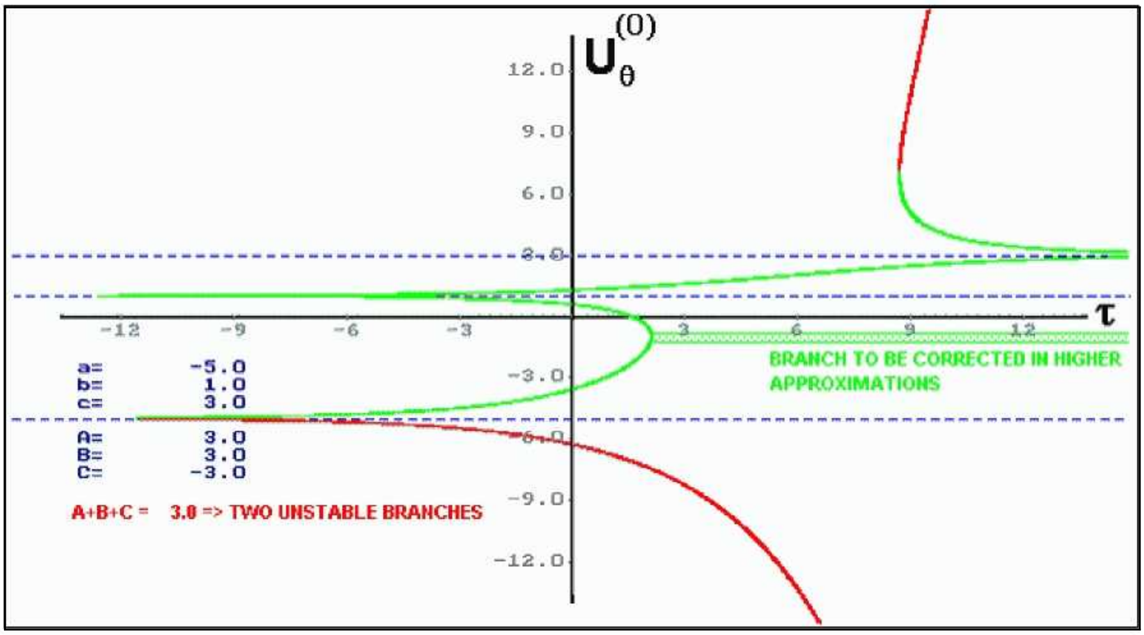

Fig. 3.1. A model calculation for $y_0(\xi,\tau,t)$ for some fixed ξ and t. Solution branches and their stability depend on the initial values taken $y_0(\xi,0,t)$. Case of three real zeros; Red branches are unstable; green ones are stable.

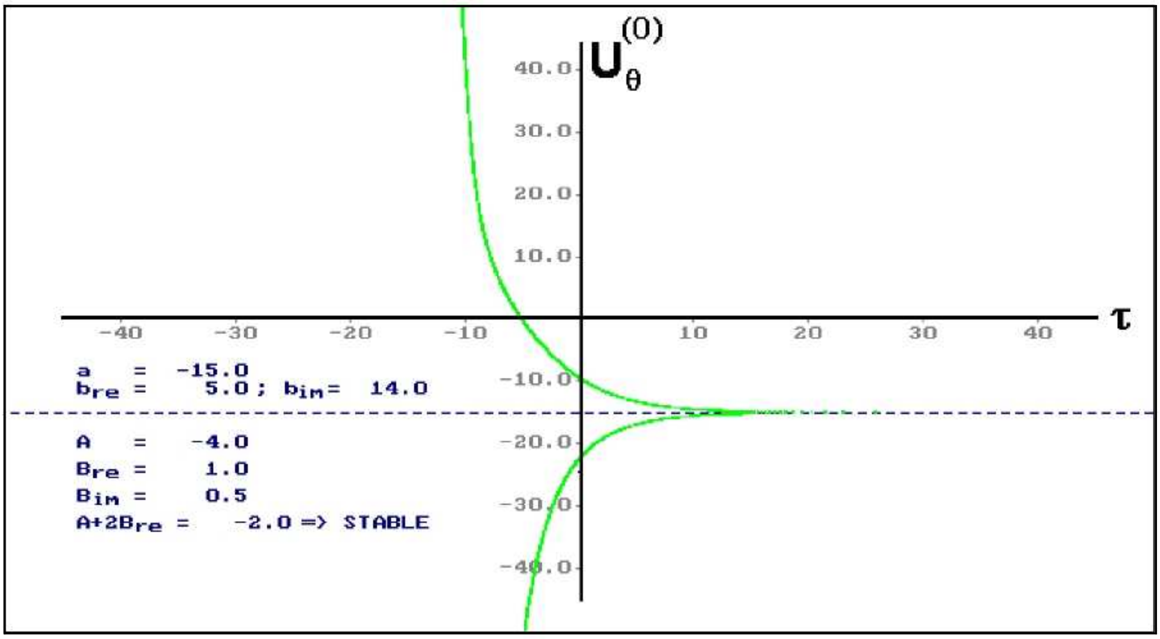

Fig. 3.2. A model calculation for $y_0(\xi,\tau,t)$ for some fixed ξ and t. Solution branches and their stability depend on the initial values taken $y_0(\xi,0,t)$. Case of one real and 2 complex conjugates zeros. Green branches are stable. No unstable branch..

4. Evolution of Toroidal Velocity

In order find the slow time evolution of $x_0(\xi,t)$, for $t>0$ and $-\infty<\xi<+\infty$, we study the following equation:

$$p_1 \frac{\partial x_0(t,\xi)}{\partial t} = \frac{\partial}{\partial \xi}\left[p_2 \frac{\partial x_0(t,\xi)}{\partial \xi} \right] + p_6\, x_0(t,\xi) + p_7 \qquad (19b")$$

where p_6 includes the effect of charge exchange, and p_7 represents the effect of the beam injection and a possible radial polarization current. This equation must be also supplemented by an initial toroidal velocity distribution along the stretched axis ξ. From the equation we note that an initial toroidal velocity will be reduced by the charge exchange collisions with neutrals.

For arbitrary temperature and density profiles and initial condition $x_0(\xi,0) = \Phi(\xi)$ $(-\infty<\xi<+\infty)$, parabolic equation (19b") has to be solved by numerical methods. It is seen that, even for a zero initial velocity distribution along ξ, $x_0(\xi,t)$ can be driven in time by the inhomogeneous terms in equation (19b") due to neutral beam injection etc.

Equation (19b") gives the slow time evolution of the toroidal velocity in the zeroth order. To this order it is decoupled from the poloidal velocity. Starting from an initial velocity distribution along the ξ - axis, it can show us the effects of individual driving terms on the r. h. s.. As the equation has position dependent coefficients, these effects are not trivial. Results of a parametrical study for two types of initial toroidal velocity distributions, i.e., a bell and a threshold shaped distributions inside the separatrix, are given in Figures 4.1 and 4.2.

In these pictures, CHX=0 means that the effect of charge exchange has been neglected. INJ=0 means no injection and INJ= -1 means that the injection is applied in the reverse direction.

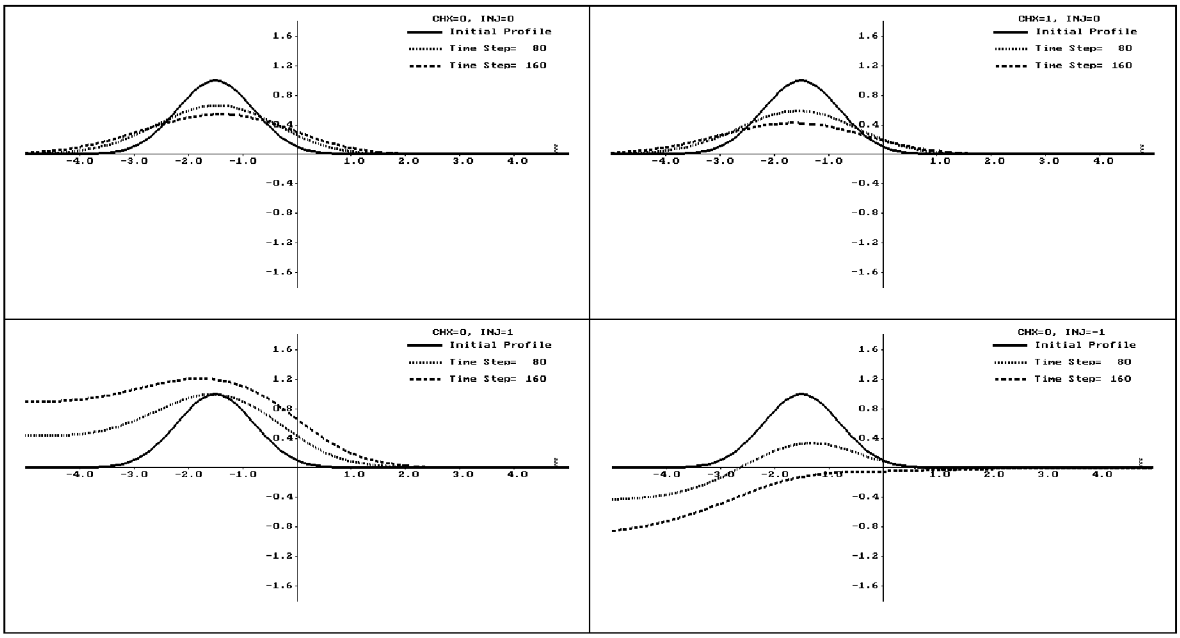

Fig. 4.1. Effects of the driving terms on the time evolution of the toroidal velocity for a bell shaped initial distribution.

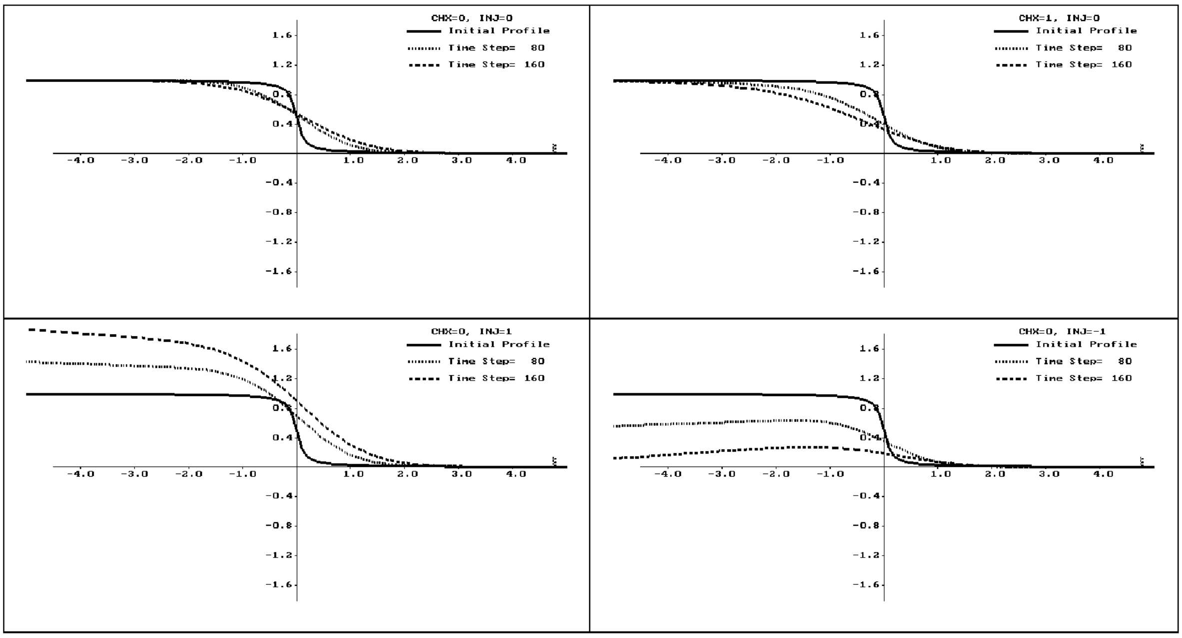

Fig. 4.2. Effects of the driving terms on the time evolution of the toroidal velocity for a threshold shaped initial distribution.

5. Description of Plasma Rotation by a Combination of Differential and Algebraic Equations

The main result of the revisited neoclassical theory [14] is an equation describing the radial transport of toroidal momentum in a collisional subsonic plasma with steep gradients:

$$\frac{1}{\eta_2}\frac{\partial}{\partial x}[\eta_2 G]=T_{CX}+T_{NBI} \tag{24}$$

G is defined by

$$G=\frac{\partial g}{\partial x}-\frac{0.107 q^2}{1+Q^2/S^2}\frac{\partial \ln T}{\partial x}\frac{B_\varphi}{B_\theta}h \tag{24a}$$

$$T_{CX}=t_{ci}\frac{\hat{N}}{\hat{\eta}_2}\nu_{cx}\, g \tag{24b}$$

accounts for the friction caused by the neutral gas and

$$T_{NBI}=t_{ci}\frac{\hat{N}}{\hat{\eta}_2\, v_T}\vec{v}_i \tag{24c}$$

for the momentum source due to neutral beam injection. The characteristic time t_{ci} at a point P_i (defined below) is given by

$$t_{ci}^{-1}=\frac{\eta_{2i}}{m_i\, N_i\, L_\psi^2} \tag{24d}$$

m_i is the ion mass, N_i the ion density at P_i,

$$L_\psi=\left|\left(\frac{\partial \ln T_i}{\partial r}\right)^{-1}\right| \tag{24e}$$

is the scale length of the ion temperature T_i at P_i. $x=(r-r_i)/L_\psi$ the radial coordinate, r_i the radius of P_i, and η_2 the perpendicular viscosity coefficient [14]. In the case of ALCATOR P_i is the 'inflection' point P_{inf} which is defined in Fig.5 as the locus of vanishing curvature of the ion temperature profile. In the case of TEXTOR (without temperature pedestal) P_i is assumed to coincide with the plasma edge ($r_i=r_s$, r_s is the minor plasma radius). G and h are the normalized and poloidally averaged toroidal and poloidal velocities,

$$g=\oint\frac{d\theta}{2\pi}\frac{U_\varphi(r,\theta)}{v_T}, \tag{24f}$$

$$h=\oint\frac{d\theta}{2\pi}\frac{U_\theta(r,\theta)}{v_T}, \tag{24g}$$

respectively. v_T is the constant positive velocity

$$v_T=\frac{1}{eB_\varphi}\frac{T_i}{L_\psi} \tag{24h}$$

e is the elementary charge. B_φ is the toroidal field and B_θ the poloidal field. The velocities Q and S are defined by [14]:

$$\frac{Q}{4v_T}=h-\hat{T}\frac{\partial \ln(N^2 T)}{\partial x}\frac{2.5}{4} \tag{24i}$$

$$\frac{S}{v_T}=\frac{8}{\Lambda'}\frac{B_\varphi}{B} \tag{24j}$$

with

$$\Lambda'=\Lambda\frac{L_T}{L_\psi}. \tag{24k}$$

The parameter Λ (crucial in the case of ALCATOR where finite Larmor radius effects are important) can be written as

$$\Lambda=\frac{\nu_i}{\Omega_i}\frac{q^2 R^2}{r L_T}. \tag{24l}$$

L_T is the radially dependent decay length

$$L_T=\left(\frac{\partial \ln T}{\partial r}\right)^{-1}, \tag{24m}$$

ν_i the ion-ion collision frequency, Ω_I the ion Larmor frequency, q the safety factor, R the major radius, $\hat{T}=T/T_i$ is the relative temperature and $\hat{N}=N/N_i$ the relative density.

Combining the ambipolarity condition with the parallel momentum equation [14] we get in the case of large aspect ratio and circular cross-section a nonlinear relation between the poloidal and toroidal plasma velocities [14].

$$\begin{aligned} h'+1.833=\frac{0.45\Lambda}{1+Q^2/S^2}T_{36}\,\tilde{v}_T\left[-\frac{B_\varphi}{B_\theta}\right]^2 \Bigg\{ & \frac{0.107q^2}{1+Q^2/S^2}h'+\frac{1}{2}\frac{1}{\left[\frac{\partial \hat{T}}{\partial x}\right]^2}(g')^2 \\ & -\frac{1}{\frac{\partial \hat{T}}{\partial x}}g'\left[h'-\left(1+\frac{2}{\eta}\right)\right]+1.9\left[h'-0.8\left(1+\frac{1.6}{\eta}\right)\right]^2\Bigg\} \end{aligned} \tag{25}$$

Here the definitions

$$g'=\frac{B_\theta}{B_\varphi}g \tag{25a}$$

$$h'=\frac{U_\theta}{\tilde{v}_T} \tag{25b}$$

and

$$\eta=\frac{L_N}{L_T} \tag{25c}$$

with

$$\tilde{v}_T = \frac{T}{eB_\varphi}\frac{\partial \ln T}{\partial r} \qquad (25d)$$

and

$$L_N = \left(\frac{\partial \ln N}{\partial r}\right)^{-1} \qquad (25e)$$

are used, to cast equation (25) in a convenient form.

5.1 Neutral beam injection

Due to neutral injection [15] the particle number N_0 increases according to

$$\dot{N}_0 = \frac{I_b\,[A]}{e_0} \qquad (26)$$

or

$$\dot{N}_0 = 0.624\times 10^{22}\,\frac{P_{MW}}{E_{keV}} \qquad (26')$$

I_b is the injected current, P_{MW} the injected power in MW and E_{keV} the beam energy in keV. We concentrate on charge exchange reactions because they leave the particle number unchanged. The rate coefficient is given by

$$<\sigma v>_{cx} = 1.5\times 10^{-13}\,\frac{m^3}{sec} \qquad (27)$$

In a radial volume element $\Delta V=(2\pi R)(2\pi r)dr$ during the time Δt the momentum

$$\Delta(m\vec{v}_i\,N_i)\Delta V = m\dot{N}_0\,\Delta t\,\frac{dl}{l_{mfp}}v_0 \qquad (28)$$

is deposited. dl is the line element along the beam path, l_{mfp} is the mean free path length due to charge exchange.

$$l_{mfp} = \frac{v_0}{<\sigma v>_{cx}\,N_i} \qquad (29)$$

Let α be the angle between the beam tangency radius R_t and the straight line R_s connecting the center point with the line element dl [15]. Then we have $dr/dl=\sin\alpha$. From the relation $\cos\alpha=R_t/R_s$ we get

$$\sin\alpha = \sqrt{2\frac{R_s - R_t}{R_s}}\,. \qquad (30)$$

Equation (28) entails

$$\vec{v}_i\,N_i = \frac{\dot{N}_0\,\dfrac{dl}{l_{lmp}}\,v_0}{2\pi R\,2\pi r\,dr}\,. \qquad (31)$$

Using mean-free-path length (29) and assuming $R_t\approx R_0$ we get

$$\vec{v}_i = \frac{\dot{N}_0 <\sigma v>_{cx}}{2\pi R\, 2\pi r \sqrt{2\varepsilon}} \tag{31'}$$

or

$$\vec{v}_i = 1.68\times 10^7 \frac{P_{MW}}{E_{keV}} \frac{m^3}{\sec^2} \frac{1}{R\, r\sqrt{\varepsilon}} \tag{31''}$$

The (dimensionless) source term is then

$$T_{NBI} = t_c \frac{\hat{N}}{\hat{\eta}_2} \frac{\vec{v}_i}{v_T}. \tag{32}$$

We note that

$$\hat{\eta}_2 = \hat{N}^2\, \hat{T}^{-\frac{1}{2}+Z} \tag{32a}$$

and therefore

$$T_{NBI} = t_c \frac{1}{\hat{N}\,\hat{T}^{-\frac{1}{2}+Z}} \frac{\vec{v}_i}{v_T}. \tag{32'}$$

5.2 Anomalous viscosity

Attempts to reproduce the rotation velocity of the L-mode TEXTOR plasma with the classical viscosity fail because the obtained velocities are much too large. Therefore, like in the case of the heat conduction, anomalous viscosity must be envisaged [16].

$$\eta_{diff} = L_\psi^2 \frac{\eta_{2,sep}}{m_i\, N_{sep}\, L_\psi^2} \tag{33}$$

$$\eta_{diff}\, m_i\, N_{sep} = \eta_{2,sep} \tag{33'}$$

Using the characteristic time τ_T

$$\eta_{diff} = L_\psi^2 \frac{1}{\tau_T} \tag{33''}$$

$$\frac{1}{\tau_T} = \frac{\eta_{diff}}{L_\psi^2} = \frac{\eta_{2,sep}}{m_i\, N_{sep}\, L_\psi^2}$$

what gives the same result. The shape of the temperature and density profiles in TEXTOR makes the ITG instability likely to be the primary candidate. The growth rage of the instability is [16]

$$\gamma_{ITG} = \frac{2T_e k_y}{eBR} \sqrt{\frac{\varepsilon_i}{<Z>}(1-0.67p) - \frac{\varepsilon_i^2 p^2}{4}}. \tag{34}$$

Here the peaking factor p is defined by

$$p = \frac{1}{\eta_i} = \frac{d\ln(N_i)}{d\ln(T_i)} \tag{34a}$$

and

$$\varepsilon_{i,e} = -\frac{R}{2}\frac{d\ln T_{i,e}}{dr} \tag{34b}$$

(The parameter η_i is normally used in ITG-instability considerations).

In the case of saturated turbulence the diffusivity is given by [16]

$$D_\perp = \frac{<<\gamma_\Sigma>>}{<<k_y>>}\alpha_D(r) \tag{35}$$

Here γ_Σ is the sum of growth rates of the excited instabilities and <<···>> denotes the average value over the region with positive growth rate. The empirical profile $\alpha_D(r)$ is chosen to be proportional $q^2(r)$ [16].

5.3 Solution method, results and discussion

Equation (24) is a second order equation for g, the normalized toroidal velocity if the definition (24a) of G is inserted. This equation is replaced by two first order equations. The first equation is obtained by resolving equation (24a) with respect to $\partial g/\partial x$.

$$\frac{\partial g}{\partial x} = G + \frac{0.107q^2}{1+Q^2/S^2}\frac{\partial \ln T}{\partial x}\frac{B_\varphi}{B_\theta}h \tag{36}$$

The second equation is that for $\partial G/\partial x$ which is (almost) identical with equation (24).

In addition we have the equation (25) for the poloidal rotation. For a given temperature, density and normalized toroidal velocity g this equation is solved for h by means of a solver for transcendental equations. We assume a symmetric streaming of the scrape-off plasma into the divertor. This yields as boundary value $h(r=r_s)=0$. We assume moreover $g(r=r_s)=0$ because of the absence of momentum sources as in the case of ALCATOR and because neutrals may be reducing $g(r=r_s)$ to a low value (in spite of NBI).

The input data are those of TEXTOR [17] and ALCATOR C-MOD [18]. The TEXTOR data are: $r_i=r_s=46$ cm, R=175 cm, $T_{imax}=1500$ eV, $T_{emax}=1200$ eV, $N_{max}=5.4\times10^{13}$ cm^{-3}, $\eta_I=1.6$, $B_\varphi=2.23$ T. NBI is characterized by $P_{MW}=0.72$, $E_{keV}=40$ (deuterons). The plasma current is $I_p=351$ kA. In the case of ALCATOR we concentrate on the temperature pedestal, which may be characterized by the data $T_i=165$ eV, $N_i=1.87\times10^{20}$ m^{-3}, $L_\psi=0.76$ cm, $r_i=20.8$ cm, $r_s=21.5$ cm. The remaining parameters are given by $\varepsilon=1.6$, $Z_{effi}=1.57$, Z=0.875, $\eta=1.6$, R=67 cm, $B_\theta=0.625$ T, $B_\varphi=5.2$ T. Here Z_{effi} and Z are defined by $Z_{eff}(r)=Z_{effi}\hat{T}^Z$, i.e., Z_{effi} is $Z_{eff}(r)$ at the inflection point.

The experimental temperature profiles of ALCATOR and TEXTOR can be seen in Fig.5.1 and Fig. 5.2, respectively. In the case of TEXTOR the total plasma cross-section is accounted for. For r>0.15 m the temperature in Fig. 5.2 decays almost linearly. In the case of ALCATOR we account for the edge pedestal only, since here the toroidal velocity jumps to its maximum value. Figs. 5.3-5.6 display TEXTOR-results. Fig. 5.3 shows the toroidal speed for vanishing neutral gas density and Fig. 5.4 the analogous curve for $N_0=4\times10^{16}$ m^{-3}. Whereas in Fig. 5.3 the toroidal speed is too large by around 50 km/sec, in

Fig. 5.4 the maximum toroidal speed $U_{\varphi max}$=110 km/sec is reproduced with an accuracy of 10%. Thus the ITG-turbulence accounts approximately for the enhancement of the classical momentum transport. The ratio of turbulent viscosity to the classical viscosity is around 100.

The radial dependence of the toroidal speed in the case of ALCATOR looks like the temperature profile of Fig. 5.1. Since the only source term is due to the temperature gradient only, the toroidal speed reaches the maximum value in the gradient region of the temperature. The level of U_φ obtained is that reported for ALCATOR (30 km/sec).

Fig. 5.5 shows the poloidal rotation speed, which is computed from neoclassical theory, is small compared to the contribution the NBI-source term, because the contribution of the respective term in equation (24) to the toroidal speed.

The radial electric field, computed from the velocity field in the case $N_0=4\times10^{16}$ m^{-3} shows (Fig. 5.6) a negative minimum at the outside. Although this minimum is only 20% of the maximum it follows qualitatively the trend of the measurements.

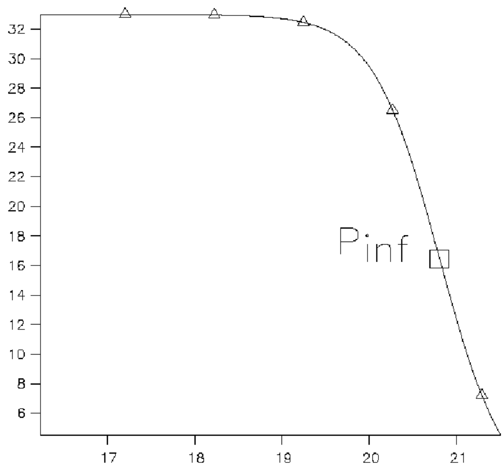

Fig. 5.1. Temperature profile (10eV) in ALCATOR C-MOD

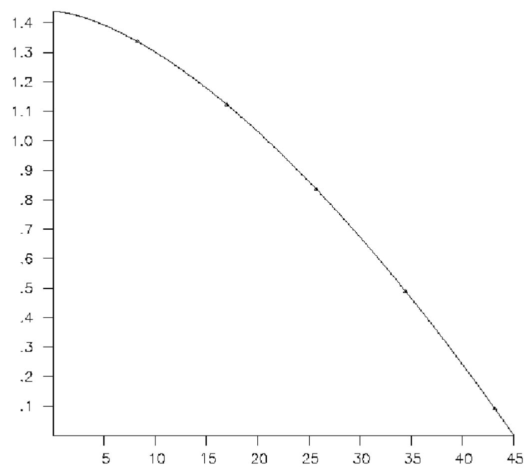

Fig. 5.2. Temperature profile (keV) in TEXTOR

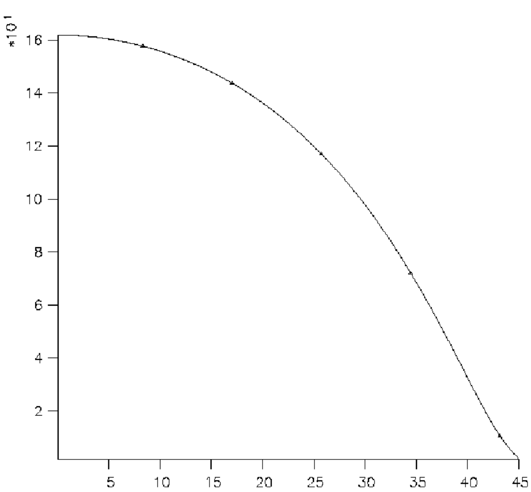

Fig. 5.3. Toroidal velocity (km/sec) in TEXTOR for $N_0=0$

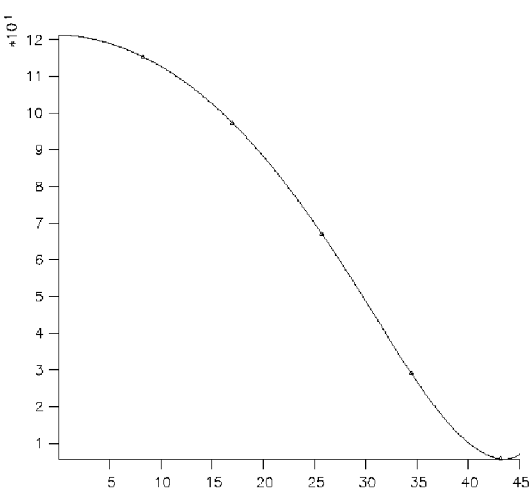

Fig. 5.4. Toroidal velocity (km/sec) in TEXTOR for $N_0=4\times10^{16}$ m^{-3}

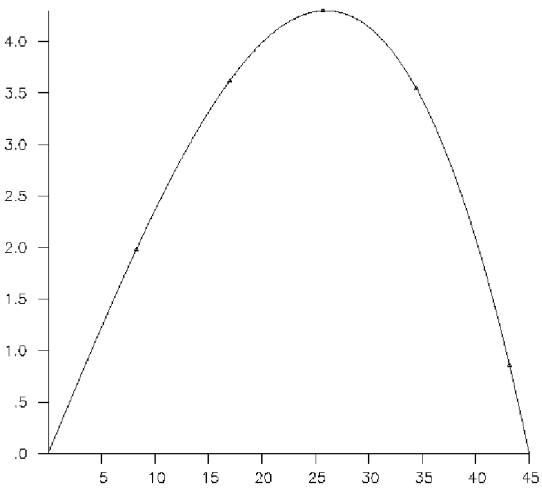

Fig. 5.5. Poloidal velocity (TEXTOR)

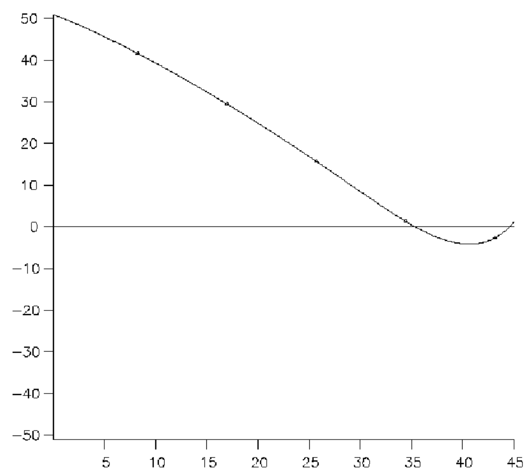

Fig. 5.6. Electric field (TEXTOR)

6. Effects of Helical Perturbations due to Saddle Coils

6.1 Plasma braking due to helical perturbations

Helical perturbation imposed by e. g. the saddle coils at JET [19, 20] modulate the absolute value of the total field

$$B = B_0(\theta)(1+\sum_{m,n} b_{m,n}(\theta,\varphi)) \tag{37}$$

B_0 is the axisymmetric Tokamak field and $b_{m,n}$ is defined by

$$b_{m,n}(\theta,\varphi) = b_{\varphi,m,n}\sin(m\theta - n\varphi + \varphi^t_{m,n}) + b_{\theta,m,n}\sin(m\theta - n\varphi + \varphi^p_{m,n}) \tag{38}$$

$b_{\varphi,m,n}$ and $b_{\theta,m,n}$ are the (relative) Fourier components of the toroidal and poloidal perturbing field, respectively. $\varphi^t_{m,n}$ and $\varphi^p_{m,n}$ are the respective phases. We get as braking term $K = \langle \vec{e}_\varphi \cdot \vec{\nabla}\overleftrightarrow{\Pi}\rangle$,where $\vec{e}_\varphi$ is the unit vector in toroidal direction and $\overleftrightarrow{\Pi}$ is the viscosity tensor accounting for the pressure anisotropization [21, 22], the expression

$$K = \frac{2\sqrt{\pi}p_i}{v_{Ti}} v_\varphi \sum_{m,n} \langle \frac{\vec{e}_\varphi \cdot \nabla B}{B} \frac{\partial b_{m,n}}{\partial \varphi} \rangle \frac{q}{|m - nq|} \tag{39}$$

which has for $q = m/n$ a singularity.

6.1.1 'Braking' time for (m=0,n) - perturbations due to mode coupling

From momentum balance (without source) we can estimate the time needed to brake down the plasma from a prescribed initial speed. From

$$m_i N_i \frac{\partial U_\varphi}{\partial t} + \langle \vec{e}_\varphi \cdot \vec{\nabla}\overleftrightarrow{\Pi}\rangle = 0 \tag{40}$$

we get, using that $K = \langle \vec{e}_\varphi \cdot \vec{\nabla}\overleftrightarrow{\Pi}\rangle$ is proportional to U_φ

$$\frac{\partial U_\varphi}{\partial t} + K' U_\varphi = 0 \tag{41}$$

Here K' is defined by $K' = \frac{K}{U_\varphi}$. The breaking time then reads

$$\tau_{br} = \frac{m_i N_i}{K'} \tag{42}$$

For the m=0 contribution we get [19]

$$\tau_{br} = \frac{m_i N_i R_0 v_{Ti}}{4\sqrt{\pi}p_i} \left(\frac{aB_\varphi}{\psi_{0,n}}\right)^2 n\varepsilon^2 \tag{43}$$

$\psi_{0,n}$ is the flux–function of the field component, ε the inverse aspect ratio. Now we assume (as a reasonable example)

$$\frac{aB_\varphi}{\psi_{0,n}} = 10^3$$

As thermal velocity we use

$$v_{Ti} = 10^4 \sqrt{\frac{T_i[eV]}{M_i}} \frac{m}{sec} \tag{44}$$

M_i is the atomic mass in AMU. This scalar pressure can be written as $P_i = N_i m_i v_{Ti}^2$ and we get as braking time due to the mode (0, n)

$$\tau_{br} = \frac{R_0}{4\sqrt{\pi}\, v_{Ti}} 10^{-6}\, n\, \varepsilon^2 = \frac{R_0[m]\sqrt{M_i}}{4\sqrt{\pi}\, 10^4 \sqrt{T_i[eV]}} 10^{-6}\, n\, \varepsilon^2$$

With the parameter set $R_0 = 3m, T_i = 2keV, \varepsilon = 0.3$ we get $\tau_{br} = 130\, msec$.

6.1.2 'Braking' time for arbitrary (m, n) – perturbations

Since the field of the perturbation coil has in general three components (linked by $\vec{\nabla}\cdot\vec{B}=0$) the total field, one has to consider the poloidal and toroidal components which contribute to the braking effect. The braking term due helical perturbations is given by [21,22]

$$K' = \frac{\sqrt{\pi}\, p_i}{v_{Ti} R_0} \sum_{m,n} \frac{(B_{0,\theta}\, b_{\theta,m,n} + B_{0,\varphi}\, b_{\varphi,m,n})^2}{B_0^{\,2}} \frac{n^2 q}{|m - nq|} \tag{45}$$

In the case of helical conductors the dominant field components are the poloidal and the radial ones, because they are both perpendicular to the direction of the conductor. However the saddle coil at JET has also an important contribution to the toroidal component originating from the conductors in the poloidal direction.

If we assume $\frac{B_{0,\theta}}{B_0} = \varepsilon_b \approx \varepsilon$ and $\frac{B_{0,\varphi}}{B_0} = 1$ we get as braking term

$$K' = \frac{\sqrt{\pi}\, p_i}{v_{Ti} R_0} \sum_{m,n} \varepsilon_b^2\, b_{\theta,m,n}^2 \left(1 + \frac{b_{\varphi,m,n}}{\varepsilon_b\, b_{\theta,m,n}}\right)^2 \frac{n^2 q}{|m - n q|} \tag{45a}$$

and the braking time

$$\tau_{br} = \frac{R_0[m]\sqrt{M_i}}{\sqrt{\pi}\, 10^4 \sqrt{T_i[eV]}} \frac{1}{\sum_{m,n} \varepsilon_b^2\, b_{\theta,m,n}^2 \left(1 + \frac{b_{\varphi,m,n}}{\varepsilon_b\, b_{\theta,m,n}}\right)^2 \frac{n^2 q}{|m - n q|}} \tag{46}$$

Assuming the parameters $R_0 = 3m, T_i = 5keV, \varepsilon = 0.3$, and the estimate $b_{\varphi,m,n} / b_{\theta,m,n} = \varepsilon_b$ we get with $b_{\theta,m,n} = 10^{-3}$ and

$$\tau_{br} = 5.4\frac{m-nq}{n^2 q}\sec$$

The main difference to the m=0 case is appearance of the resonant denominator in the source term. The large τ_{br} outside the rational surfaces means that the braking is only important at these surfaces.

6.1.3 Treatment of the singularity

The singular denominator in the preceding source term needs a careful treatment in the numerical approach. With a Taylor expansion around the singular surface we get

$$\frac{1}{m-nq} = \frac{1}{n\left(\frac{m}{n}-q\right)} = \frac{-1}{n\frac{dq}{dr}(r-r_s)}$$

Here r_s is the radius of the surface q=m/n. By physical reasons discussed below, the singularity must be replaced by

$$f_{sing_1}(r) = \frac{1}{|r-r_s|},\ \text{for } |r-r_s| \geq \varepsilon_0 \tag{47a}$$

and

$$f_{sing_1}(r) = \frac{1}{\varepsilon_0},\ \text{for} |r-r_s| \langle \varepsilon_0 . \tag{47b}$$

We approximate this radial dependence by a function typical for resonances

$$f_{sing_2} = A\frac{1}{\sqrt{(r-r_s)^2+\varepsilon_3^2}} \tag{48}$$

ε_3 is a small length allowing a numerical treatment.The amplitude A is determined from the condition that the total integrated source given by both source functions should be equal.

$$\int_{r_s-\varepsilon_1}^{r_s+\varepsilon_2} f_{sing_1}\,dr = \int_{r_s-\varepsilon_1}^{r_s+\varepsilon_2} f_{sing_2}\,dr \tag{49}$$

where ε_1 and ε_2 are the distances from the singular surfaces whose numbers are 1 and 2, respectively. We assume that for r_s-,$_1$<r< r_s+,$_2$ the collision dominated regime is entered where $1/(r-r_s)$ is to be replaced by $1/\varepsilon_0$. We get, assuming r_s=0

$$\int_{r_s-\varepsilon_2}^{r_s+\varepsilon_2} f_{sing_1}\,dr = \int_{-\varepsilon_1}^{-\varepsilon_0}\frac{1}{|x|}dx + \left.\frac{x}{\varepsilon}\right|_{-\varepsilon_0}^{\varepsilon_0} + \int_{\varepsilon_0}^{\varepsilon_2}\frac{1}{|x|}dx = \ln\left(\frac{\varepsilon_1\varepsilon_2}{\varepsilon_0^2}\right)+2 \tag{50}$$

Using the relation

$$\int\frac{dx}{x^2+\varepsilon_0^2} = \ln(x+\sqrt{x^2+\varepsilon_0^2}). \tag{52}$$

we have

$$A\int_{-\varepsilon_2}^{\varepsilon_1}\frac{dx}{\sqrt{x^2+\varepsilon_3^2}}=A\ln(\varepsilon_2+\sqrt{\varepsilon_2^2+\varepsilon_3^2})-\ln(\varepsilon_1+\sqrt{\varepsilon_2^2+\varepsilon_3^2}) \tag{53}$$

Thus we get from equation (49)

$$\mathrm{A}\ln\frac{\varepsilon_2+\sqrt{\varepsilon_2^2+\varepsilon_3^2}}{-\varepsilon_1+\sqrt{\varepsilon_1^2+\varepsilon_3^2}}=\ln\frac{\varepsilon_1\varepsilon_2}{\varepsilon_0^2}+2 \tag{54}$$

Since ε_3 is small we can write

$$\mathrm{A}\ln\frac{\varepsilon_2+\varepsilon_2\sqrt{1+\frac{\varepsilon_3^2}{\varepsilon_2^2}}}{-\varepsilon_1+\varepsilon_1\sqrt{1+\frac{\varepsilon_3^2}{\varepsilon_1^2}}}=\ln\frac{\varepsilon_1\varepsilon_2}{\varepsilon_0^2}+2 \tag{55}$$

By expansion we get

$$\mathrm{A}\ln\frac{\varepsilon_2+\varepsilon_2\left(1+0.5\frac{\varepsilon_3^2}{\varepsilon_2^2}\right)}{0.5\frac{\varepsilon_3^2}{\varepsilon_1^2}}=\ln\frac{\varepsilon_1\varepsilon_2}{\varepsilon_0^2}+2 \tag{56}$$

and by simplifying

$$\mathrm{A}\ln\frac{4\varepsilon_2+\frac{\varepsilon_3^2}{\varepsilon_2}}{\frac{\varepsilon_3^2}{\varepsilon_1}}=\ln\frac{\varepsilon_1\varepsilon_2}{\varepsilon_0^2}+2 \tag{56'}$$

or

$$\mathrm{A}\ln\frac{4\varepsilon_2\varepsilon_1+\frac{\varepsilon_3^2\varepsilon_1}{\varepsilon_2^2}}{\varepsilon_3^2}=\ln\frac{\varepsilon_1\varepsilon_2}{\varepsilon_0^2}+2 \tag{56''}$$

Since ε_3 is much smaller than $\varepsilon_{1,2}$, we obtain

$$\mathrm{A}\ln\frac{4\varepsilon_1\varepsilon_2}{\varepsilon_3^2}=\ln\frac{\varepsilon_1\varepsilon_2}{\varepsilon_0^2}+2 \tag{57}$$

We assume $\varepsilon_1=\varepsilon_2$ and can write

$$\mathrm{A}\ln\frac{2\varepsilon_1}{\varepsilon_3}=\ln\frac{\varepsilon_1}{\varepsilon_0}+1 \tag{58}$$

with 1=ln(e) we get

$$\left[\frac{2\varepsilon_1}{\varepsilon_3}\right]^{\mathrm{A}}=\frac{e\varepsilon_1}{\varepsilon_0} \tag{59}$$

or

$$e\left[\frac{\varepsilon_3}{2\varepsilon_1}\right]^A=\varepsilon_0 \tag{59a}$$

We assume e. g. A=10, $\varepsilon_3=10^{-4}$, $\varepsilon_1=10^{-3}$ and get for ε the very small number

$$\varepsilon_0=e\left[\frac{1}{20}\right]^{10}=3\frac{1}{1024}10^{-10}$$

This, however, is not confirmed by the following considerations:

An estimate of ε can be inferred from the condition that the plasma has to be in the plateau regime. We assume the temperature T=5 keV and the density N = 6×10^{13} cm^{-3}. Then we get the collision frequency ν_i = 100 sec^{-1} and the thermal speed α_i = 10^6 m/sec. The condition for being in the plateau regime is

$$\omega_{T,i} \geq \nu_i$$

Here $\omega_{T,i}$ is the transit frequency defined by

$$\omega_{T,i}=2\pi\ \alpha_i\ /L_{hel}$$

L_{hel} is is the fieldline length between two neighbouring magnetic wells. The aforementioned condition can be rewritten as

$$L_{hel} \leq \lambda_{mfp}$$

Where λ_{mfp} is the mean free path length. Thus we have the upper limit

$$L_{hel} \leq 10^6/100=10^4$$

A nonresonant surface is still in the plateau regime, if if the path length L_{hel} between two magnetic wells is smaller then the mean free path length. Since L_{hel} becomes infinite at the resonant surface, the particles at this surface are in the collision dominated regime. The angle $\Delta\iota$ by which a field line must be turned (in going away from the resonant surface) to obtain this length between the magnetic wells is given by

$$\Delta\iota\lambda_{mfp}=\frac{2\pi r_s}{m} \tag{60}$$

or

$$\Delta\iota=\frac{2\pi r_s}{m\lambda_{mfp}} \tag{60a}$$

Since we have the relation $q=2\pi/\iota$ and therfore

$$\Delta q=-\frac{2\pi}{\iota^2}\Delta\iota \tag{61}$$

we get

$$\frac{dq}{dr}(r-r_s)=1.6\times10^{-4}$$

Thus we obtain as distance from the resonant surface (for reaching the plateau regime)

$$|r - r_s| > \frac{1.6\times10^{-4}}{\frac{dq}{dr}} \approx 10^{-4}\ \mathrm{m}$$

i.e. smaller than the Larmor radius.

6.1.4 Toroidal speed of magnetic field structure

A point with constant phase is given by

$$m\theta - m\varphi + \omega t = \text{const.}$$

In the plane φ=const the structure revolves with

$$\dot{\theta} = \omega / m$$

and in the coordinate surface θ=const the structure revolves with $\dot{\varphi} = \omega / n$. Thus, with e.g. the frequency $\nu_{power}=10^4\ \mathrm{sec}^{-1}$ (TEXTOR) we get the toroidal velocity

$$v_t = \frac{\omega}{n} R_0 = \frac{\nu_{power}}{n} 2\pi R_0 = \frac{10^4}{2} 2\pi R_0 = 55\,\mathrm{km/sec}$$

if we concentrate on m=6, n=2 and take R_0=1.75 m.

6.1.5 Fourier analysis of the magnetic field of the saddle coils

By means of the winding generator in FLOC [23] four loops are generated (Figs. 6.1, 6.2) which represent within some accuracy the saddle coils at JET. Since the lower Fourier components are rather insensitive with respect to the geometrical details, the simplifications with respect to the real configuration should be tolerable.

Two current configurations, given in Fig. 6.1 and 6.2, respectively, had been envisaged: in Fig. 6.1 the currents are antiparallel in adjacent windings, what favorizes the n=2 components. In Fig. 6.2 the currents in two adjacent coil pairs are parallel, but opposite in the two pairs. The current in all coils is 10 kA.

The Fourier components are computed the q=2 surface. For the adjacent q=3 and q=4 surfaces the components must in principle be recalculated.

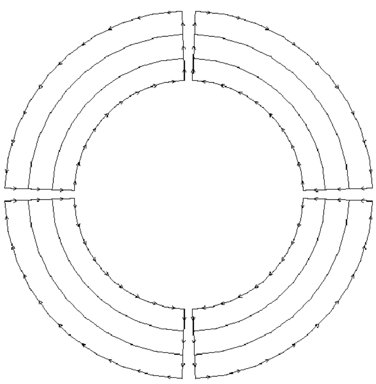

Fig. 6.1 Parallel currents in adjacent windings

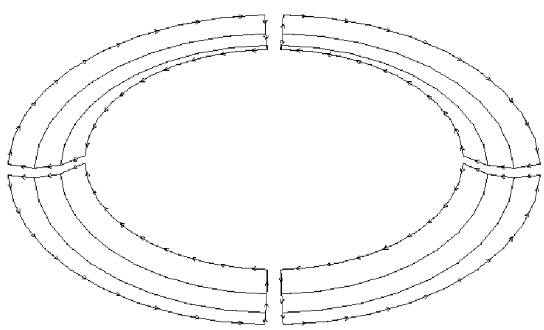

Fig. 6.2 Antiparallel currents in adjacent windings

6.2 Results

The input data are those of TEXTOR and JET. The Textor data (shot #91269) are: $r_i = r_s =$ 46 cm, R=175 cm, T_{imax} = 1500 eV, T_{emax} = 1200 eV, $N_{max} = 5.4 \times 10^{13}$ cm^{-3}, η_i = 1.6, B_φ = 2.23 T. NBI is characterized by P_{MW} = 0.72, E_{keV} = 40 (deuterons). The plasma current is I_p = 350 kA. The choice of the JET data correspond to shot #53298: major radius R=296 cm, minor half axis r=110 cm, T_{imax} = 3 keV, $N_{max} = 8 \times 10^{13}$ cm^{-3}, η_i =1.6, B_φ = 2.3 T. NBI is charaterized by P_{MW} = 3 MW, E_{keV} = 80 (deuterons). The plasma current is I_p = 3.5 MA.

The toroidal velocity (Fig. 6.3 for TEXTOR and Fig. 6.4 for JET) shows at the resonant surface, which is located at 25 cm (Textor) and 70 cm (JET) a local minimumdue to the braking term.

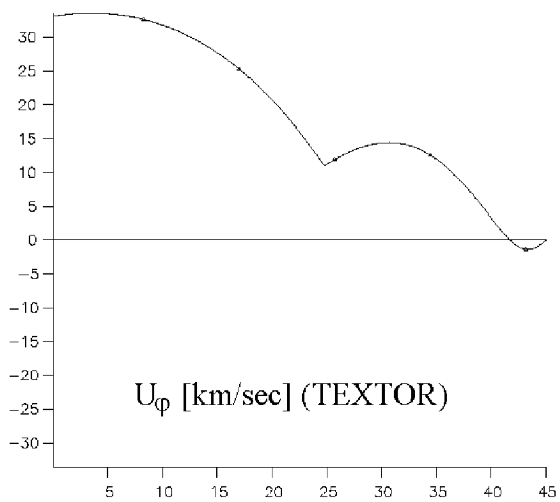

Fig. 6.3 Toroidal velocity distribution in TEXTOR

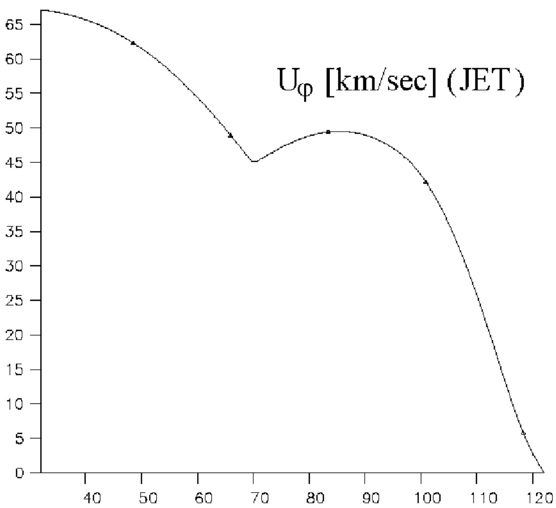

Fig. 6.4 Toroidal velocity distribution in JET

Figs. 6.5 and 6.6 are devoted to the Fourier analysis of the magnetic field of the saddle coils, which are depicted in Figs. 6.1 and 6.2

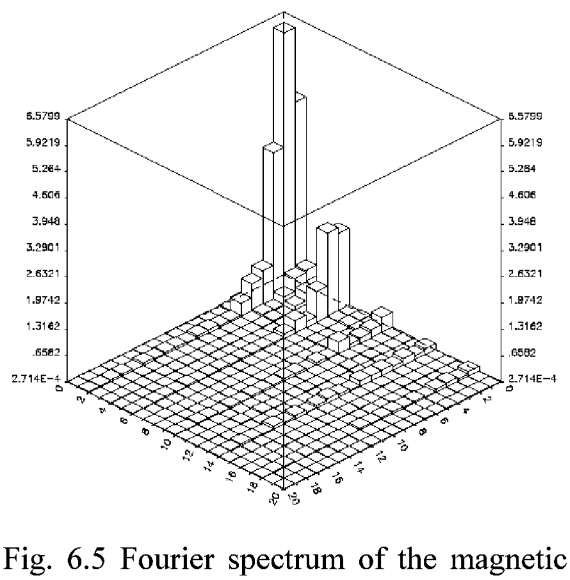

Fig. 6.5 Fourier spectrum of the magnetic field of the parallel currents in saddle coils

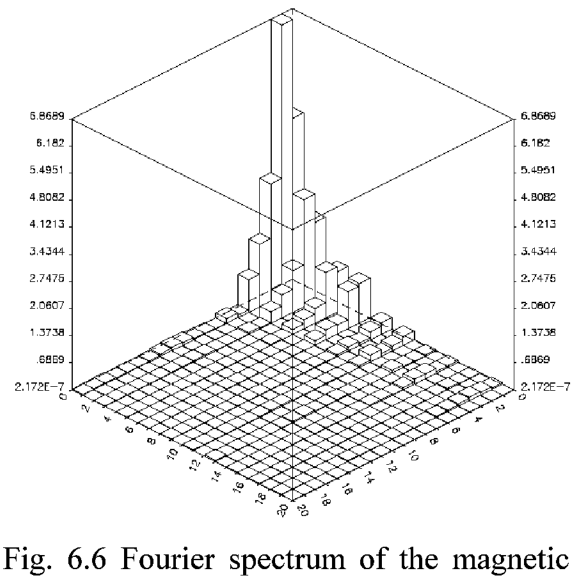

Fig. 6.6 Fourier spectrum of the magnetic field of the antiparallel currents in saddle coils

Fig. 6.5 shows the spectrum of the configuration in Fig. 6.1. Since the current is alternating from one coil to the next, the maximum components are those with n=2. (The axis on the right side of the figure is the n - axis and that on the left side the m - axis) The components decrease sharply with increasing m. The harmonics at n=6 and n = 10 are unimportant, because they can hardly be resonant.

Fig. 6.6 shows the spectrum of the configuration in Fig. 6.2. Now we get the dominant components for n=1. $B_{m=2,\, n=1} \approx 6.5$ G is the main candidate to produce a sufficiently large shearing rate.

According to [19] the braking term must be increased by a factor $646/q^2$ to account for the '1/ν' – regime. Equivalent to this is an increase of the Fourier components by a factor $25.4/q \approx 10$. Thus the relative strength of the perturbation is $b_{\theta 2,1}/B_0 \approx 3 \times 10^{-3}$.

In the case of Textor the Fourier analysis shows that the effective relative perturbation is $b_{\theta 2,1}/B_0 \approx 7 \times 10^{-2}$. Introducing the counter rotation of the magnetic field structure, the minima shown in Figs. 6.3, 6.4 can be pushed to the x – axis [24].

6.3 Discussion

The calculations show that there is a considerable impact of the helical perturbations on the rotation velocity. In particular rotating fields should have the ability not only to brake the rotation but also the revert the sign of the rotation speed. The Fourier analysis shows that in the case of the saddle coils at JET n=1 – modes appear. Thus the m=2 – mode can used to influence the rotation velocity at the q=2 surface. In spite of singularity in the braking term it seems to be impossible to produce a strong gradient in the rotation field leading to an ITB. By counterrotating the magnetic field structure this gradient could be strongly increased.

Appendix A. Outline of the Derivation of Toroidal and Poloidal Momentum Equations

In this Appendix, starting from the Braginskii's equations, the outline of the derivation of toroidal and parallel momentum equations will be presented from the perspective of the revisited neoclassical theory.

A.1 Conservation equations

Continuity Equation:

$$\frac{\partial N_j}{\partial t}+\vec{\nabla}\cdot(N_j\vec{U}_j)=0 \tag{A1}$$

Momentum Equation:

$$m_j N_j \frac{d\vec{U}_j}{dt}=-\vec{\nabla}P_j-\vec{\nabla}\cdot\vec{\Pi}_j+e_j N_j(\vec{E}+\vec{U}_j\times\vec{B})+\vec{R}_j \tag{A2}$$

where $\vec{R}_j$ is the momentum transfer term, i.e. friction force, between the species. The superscripts M refer to momentum. $P_j=N_jT_j$, $\vec{\Pi}_j$, and $\vec{q}_j$ are the pressure, stress tensor and heat flux, respectively. R_j terms are relating to collisional energy transfer and frictional heating. The plasma will be assumed to consist of two fluids, i.e., electrons (j = e) and ions (j = i). Relations between $\vec{\Pi}_j,\vec{q}_j,\vec{R}_j$ and $N_j,T_j,\vec{U}_j$ can be found by means of a closure of the kinetic equations.

A.2 Stress tensors

Using the expansion of Braginskii, the stress tensor can be written as

$$\overleftrightarrow{\Pi}_j=\overleftrightarrow{\Pi}_{0,j}+\overleftrightarrow{\Pi}_{1,j}+\overleftrightarrow{\Pi}_{2,j}+\overleftrightarrow{\Pi}_{3,j}+\overleftrightarrow{\Pi}_{4,j}, \tag{A3}$$

where $\overleftrightarrow{\Pi}_{0,j}$ refers to the parallel stress tensor; $\overleftrightarrow{\Pi}_{1,j}$ and $\overleftrightarrow{\Pi}_{2,j}$, the perpendicular stress tensors, describe the effects of collisions on the Larmor orbits; $\overleftrightarrow{\Pi}_{3,j}$ and $\overleftrightarrow{\Pi}_{4,j}$, gyro-stress (gyro-viscosity) tensors, describe the finite Larmor radius effects. In the strong magnetic field ($\nu_i \ll \Omega_i$), these tensors take the following forms:

$$\begin{aligned}\overleftrightarrow{\Pi}_{0,j}=&-\eta_{0,j}(3\hat{n}\hat{n}-\overleftrightarrow{I})[\hat{n}\cdot\vec{\nabla}\vec{U}_j\cdot\hat{n}-(1/3)\vec{\nabla}\cdot\vec{U}_j\\&+(2/5P_j)\hat{n}\cdot\vec{\nabla}\vec{q}_j\cdot\hat{n}-(1/3)\vec{\nabla}\cdot\vec{q}_j]\\&-1.84\eta_{0,j}(2/5P_j)(\hat{n}\hat{n}-(1/3)\overleftrightarrow{I})[\hat{n}\cdot\vec{\nabla}(\vec{q}_j-\vec{q}_j^{*})\cdot\hat{n}\\&-(1/3)\vec{\nabla}\cdot(\vec{q}_j-\vec{q}_j^{*})+(1/3)\vec{q}_j\cdot\vec{\nabla}\ln P_j-(2/3)\vec{q}_j\cdot\vec{\nabla}\ln T_j]\end{aligned} \tag{A3a}$$

$$\begin{aligned}\overleftrightarrow{\Pi}_{1,j}=-\eta_{1,j}\{&(\hat{p}\hat{p}-\hat{b}\hat{b})[\hat{p}\cdot\vec{\nabla}\vec{U}_j\cdot\hat{p}-\hat{b}\cdot\vec{\nabla}\vec{U}_j\cdot\hat{b}+0.4P_j(\hat{p}\cdot\vec{\nabla}\vec{q}_j\cdot\hat{p}-\hat{b}\cdot\vec{\nabla}\vec{q}_j\cdot\hat{b})]\\&+(\hat{p}\hat{b}+\hat{b}\hat{p})[\hat{p}\cdot\vec{\nabla}\vec{U}_j\cdot\hat{b}+\hat{b}\cdot\vec{\nabla}\vec{U}_j\cdot\hat{p}+0.4P_j(\hat{p}\cdot\vec{\nabla}\vec{q}_j\cdot\hat{b}+\hat{b}\cdot\vec{\nabla}\vec{q}_j\cdot\hat{p})]\}\end{aligned} \tag{A3b}$$

$$\vec{\vec{\Pi}}_{2,j} = -\eta_{2,j}\{(\hat{p}\hat{n}+\hat{n}\hat{p})[\hat{p}\cdot\vec{\nabla}\vec{U}_j\cdot\hat{n}+\hat{n}\cdot\vec{\nabla}\vec{U}_j\cdot\hat{p}+0.4P_j(\hat{p}\cdot\vec{\nabla}\vec{q}_j\cdot\hat{n}+\hat{n}\cdot\vec{\nabla}\vec{q}_j\cdot\hat{p}] \\ +(\hat{b}\hat{n}+\hat{n}\hat{b})[\hat{b}\cdot\vec{\nabla}\vec{U}_j\cdot\hat{n}+\hat{n}\cdot\vec{\nabla}\vec{U}_j\cdot\hat{b}+0.4P_j(\hat{b}\cdot\vec{\nabla}\vec{q}_j\cdot\hat{n}+\hat{n}\cdot\vec{\nabla}\vec{q}_j\cdot\hat{b})]\} \tag{A3c}$$

$$\vec{\vec{\Pi}}_{3,j} = -\eta_{3,j}\{(\hat{p}\hat{p}-\hat{b}\hat{b})[\hat{b}\cdot\vec{\nabla}\vec{U}_j\cdot\hat{p}+\hat{p}\cdot\vec{\nabla}\vec{U}_j\cdot\hat{b}+0.4P_j(\hat{b}\cdot\vec{\nabla}\vec{q}_j\cdot\hat{p}+\hat{p}\cdot\vec{\nabla}\vec{q}_j\cdot\hat{b})] \\ -(\hat{p}\hat{b}+\hat{b}\hat{p})[\hat{p}\cdot\vec{\nabla}\vec{U}_j\cdot\hat{p}-\hat{b}\cdot\vec{\nabla}\vec{U}_j\cdot\hat{b}+0.4P_j(\hat{p}\cdot\vec{\nabla}\vec{q}_j\cdot\hat{p}-\hat{b}\cdot\vec{\nabla}\vec{q}_j\cdot\hat{b})]\} \tag{A3d}$$

$$\vec{\vec{\Pi}}_{4,j} = -\eta_{4,j}\{(\hat{p}\hat{n}+\hat{n}\hat{p})[\hat{b}\cdot\vec{\nabla}\vec{U}_j\cdot\hat{n}+\hat{n}\cdot\vec{\nabla}\vec{U}_j\cdot\hat{b}+0.4P_j(\hat{b}\cdot\vec{\nabla}\vec{q}_j\cdot\hat{n}+\hat{n}\cdot\vec{\nabla}\vec{q}_j\cdot\hat{b})] \\ -(\hat{b}\hat{n}+\hat{n}\hat{b})[\hat{p}\cdot\vec{\nabla}\vec{U}_j\cdot\hat{n}+\hat{n}\cdot\vec{\nabla}\vec{U}_j\cdot\hat{p}+0.4P_j(\hat{p}\cdot\vec{\nabla}\vec{q}_j\cdot\hat{n}+\hat{n}\cdot\vec{\nabla}\vec{q}_j\cdot\hat{p})]\} \tag{A3e}$$

where

$$\eta_{0,j} = \alpha_{0j} N_j T_j \tau_j \;\; ; \;\; \alpha_{0i} = 0.96 \;\; , \;\; \alpha_{0e} = 0.73 \tag{A4a}$$

$$\eta_{1,j} = \alpha_{1j} \frac{N_j T_j}{\Omega_j^2 \tau_j} \;\; , \;\; \eta_{2,j} = 4\eta_{1,j} \;\; ; \;\; \alpha_{1i} = 0.30 \;\; , \;\; \alpha_{1e} = 0.51 \tag{A4b}$$

$$\eta_{3,j} = \alpha_{3j} \frac{N_j T_j}{\Omega_j} \;\; , \;\; \eta_{4,j} = 2\eta_{1,j} \;\; ; \;\; \alpha_{3i} = 0.50 \;\; , \;\; \alpha_{3e} = -0.50 \tag{A4c}$$

τ_i and τ_e are the ion-ion and the electron-ion collision times, respectively; $\hat{p}, \hat{b}, \hat{n}$ are the orthogonal unit vectors of the curvilinear coordinate system. Details of this coordinate system will be presented in the next subchapter. In the tensor expressions, the terms including heat flux vector, $\vec{q}_j$, are the Mikhailovskii-Tsypin correction terms to the Braginskii's equations. Indeed, by using a multi-moment and a drift-kinetic approach, Mikhailovskii and Tsypin [9] have found some additional terms that modify the viscosity tensor and heat flux due to the mutual influences of the heat flux on the viscosity and the viscosity on the heat flux. The importance of these terms has been noted by Rogister [15] as follows: In the limit of

$$\Lambda_1 = \frac{0.255}{\Omega_i \tau_i} \frac{q^2 R^2}{r L_{T,i}} \to 0$$

where $L_{T,i}$ is the length scale for ion temperature gradient, Braginskii's expression leads without these terms, to $U_{\theta,i} = 0$ for the ion poloidal velocity, i.e., overestimating the contribution of the gyro-viscosity. However, a kinetic analysis [25] gives a finite ion poloidal velocity. This contradiction disappears when the indicated terms are included.

A.3 Heat flux

Heat flux vector for ions is:

$$\vec{q}_i = -\frac{P_i}{m_i}\left[\frac{3.9}{\nu_i}\hat{n}\hat{n}\cdot\vec{\nabla}T_i - \frac{5}{2}\frac{1}{\Omega_i}\hat{n}\times\vec{\nabla}T_i - 2\frac{\nu_i}{\Omega_i^2}\hat{n}\times(\hat{n}\times\vec{\nabla}T_i)\right] \tag{A5}$$

Heat flux vector for electrons consists of two parts:

$$\vec{q}_e = \vec{q}_{eu} + \vec{q}_{eT} \tag{A6}$$

Where the heat flux due to the fluid velocity of the electrons and heat flux due to the temperature gradients are following,

$$\vec{q}_{eU} = P_e \left[0.71 \hat{n}\hat{n}\cdot\vec{U}_e + \frac{3}{2}\frac{1}{\Omega_e \tau_e}\hat{n}\times\vec{U}_e \right] \tag{A6a}$$

$$\vec{q}_{eT} = \frac{P_e \tau_e}{m_e}\left[-3.16\hat{n}\hat{n}\cdot\vec{\nabla}T_e + \frac{4.66}{\Omega_e^2 \tau_e^2}\hat{n}\times(\hat{n}\times\vec{\nabla}T_e) - \frac{5}{2}\frac{1}{|\Omega_e \tau_e|}\hat{n}\times\vec{\nabla}T_e \right] \tag{A6b}$$

Finally,

$$\vec{q}_j^{\,*} = \frac{25}{24}\frac{P_j}{m_j \nu_j}\hat{n}\hat{n}\cdot\vec{\nabla}T_j \tag{A7}$$

A.4 Ordering scheme

Rogister [6] criticized the appropriateness of the existing neoclassical theories, to describe the plasma motion in the edge region, the outermost thin layer of the plasma body where the gradients are steeper comparing to the core, and the temperatures are low. His remarks are based on the following arguments.

The standard neoclassical theory assumes just a single characteristic length scale for the macroscopic lengths, qR (connection length; ranging between 6-20 m), r (minor radius; ranging between 0.5-3 m), L_T and L_N (the temperature and density gradient length scales defined by $(\partial \ln T/\partial r)^{-1}$ and $(\partial \ln N/\partial r)^{-1}$, respectively; ranging in a few centimeters). This assumption leads to the neglection of the effect of the gyro-stresses (represented by Braginskii's third and fourth stress tensors) and inertia comparing to that of parallel stress (represented by Braginskii's zeroth stress tensor) [6].

This hypothesis is acceptable in the following limits:

$$\Lambda_1 \equiv \frac{0.255}{\Omega_i \tau_i}\frac{q^2 R^2}{r L_{T,i}} \to 0 \quad \text{and} \quad \Lambda_2 \equiv \left(\frac{m_e}{m_i}\right)^{1/2}\left(\frac{qR\nu_i}{c_i}\right)^2 \to 0$$

where $\nu_i = 1/\tau_i$ is the ion-ion collision frequency.

Λ_1 represents the ratio of the effect of the gyro-viscosity across the magnetic surfaces to that of the viscosity along the field lines. Λ_2 is the ratio of the parallel ion heat diffusion time scale to the electron-ion energy equi-partition time scale [26].

However, in the high collisionality regime, one has $\hat{\nu}_j = qR\nu_j/c_j \gg 1$, and in the case of $\Lambda_1 \sim 1, \Lambda_2 \sim 1$, which is generally the case at the plasma edge, gyro-stresses can modify the energy and parallel momentum equations. In order to remove the above-mentioned weaknesses of the standard neoclassical theory, Rogister [6] has proposed a different scaling of the parameters for the collisional plasma edge region with steep gradients.

In order to obtain the parallel momentum equation via a regular perturbation expansion, we shall apply below the Rogister's scaling. Depending on the fact $L_\psi \ll r \ll qR$, where L_ψ is the radial gradient length scale, the ordering scheme for large aspect ratio approximation is given as follows:

$$\frac{1}{\hat{\nu}_j} \sim \frac{L_\psi}{r} \sim \frac{r}{qR} \sim \mu; \quad \frac{e_j \upsilon}{T_j} \sim \frac{a_i}{L_\psi} \sim \left(\frac{m_e}{m_i}\right)^{1/2} \sim \mu^2 \tag{A8}$$

where $\mu \sim 0.1$ is the expansion parameter, υ is the loop voltage induced by the transformer to drive the tokamak toroidal current and $a_i = c_i / \Omega_i$ is the ion Larmor radius. For tokamak devices, the following ordering for the magnetic field components is suitable:

$$B_\chi \sim \mu B; \; B_\varphi \sim B \tag{A9}$$

Although, in leading order, the radial velocities, $U_{\psi,i} = \vec{U}_i \cdot \hat{p} = \vec{U}_i \cdot \hat{e}_\psi$, resulting from the poloidal gradients, are of the order of $\mu^4 c_i$, since

$$U_{\psi,j} \sim \varepsilon \frac{T_j}{eB} \frac{1}{r} \sim \mu^4 c_i \tag{A10a}$$

However, in obtaining flux-surface-averaged equations for electron conservation, since dominant and first order terms involving the radial velocities cancel out, $U_{\psi,j}$ drops by two orders of magnitude [6] and become

$$U_{\psi,j} \sim \mu^6 c_i \tag{A10a'}$$

The diamagnetic velocity, $U_{\beta,i} = \vec{U}_i \cdot \hat{b}$, in the binormal direction was taken at the order of $\mu^2 c_i$ since

$$U_{\beta,j} \sim \varepsilon \frac{T_j}{eB} \frac{1}{L_\psi} \sim \mu^2 c_i \tag{A10b}$$

The relative electron-ion mean velocity along the field lines $U_{\|,e\text{-}i}$ is at the order of $e\upsilon / 2\pi R m_e \nu_e$. Since the high collisionality causes the velocities of the species to be at the same order, the parallel velocity, $U_{\|,i} = \vec{U}_i \cdot \hat{n}$, of the species is found to be at the order of μc_i.

$$U_{\|,j} \sim U_{\|,e-i} \sim \frac{e\upsilon}{T_e} \left(\frac{2\pi R \nu_e}{c_e} \right)^{-1} c_e \sim \mu c_i \tag{A10c}$$

The poloidal velocity, $U_{\chi,i} = \vec{U}_i \cdot \hat{e}_\chi$, is at the order of the binormal velocity, since

$$U_{\chi,j} = \frac{B_\varphi}{B} U_{\beta,j} + \frac{B_\chi}{B} U_{\|,j} \sim 1 \cdot (\mu^2 c_i) + \mu(\mu c_i) \sim \mu^2 c_i \tag{A10d}$$

And finally, the toroidal velocity, $U_{\varphi,i} = \vec{U}_i \cdot \hat{e}_\varphi$, scales as the parallel velocity since,

$$U_{\varphi,j} = \frac{B_\varphi}{B} U_{\|,j} - \frac{B_\chi}{B} U_{\beta,j} \sim 1 \cdot (\mu c_i) + \mu(\mu^2 c_i) \sim \mu c_i \tag{A10e}$$

The velocity components can be expanded as follows:

$$U_{\psi,i} = U_{\psi,i}^{(6)}(\psi) + U_{\psi,i}^{(7)}(\psi,\chi); \; U_{\psi,i}^{(7)} \sim \mu U_{\psi,i}^{(6)} \tag{A11a}$$

$$U_{\chi,i} = U^{(2)}_{\chi,i}(\psi) + U^{(3)}_{\chi,i}(\psi,\chi);\; U^{(3)}_{\chi,i} \sim \mu U^{(2)}_{\chi,i} \tag{A11b}$$

$$U_{\varphi,i} = U^{(1)}_{\varphi,i}(\psi) + U^{(2)}_{\varphi,i}(\psi,\chi);\; U^{(2)}_{\varphi,i} \sim \mu U^{(1)}_{\varphi,i} \tag{A11c}$$

where the superscript in parenthesis denotes the order of the velocity in terms of μ.

Various quantities can be written as below:

$$P_i = P_i^{(0)}(1+p_i^{(1)});\; N_i = N_i^{(0)}(1+n_i^{(1)});\; T_i = T_i^{(0)}(1+t_i^{(1)}) \tag{A12a}$$

$$h_\psi = h_\psi^{(0)}(1+h_\psi^{(1)});\; h_\chi = h_\chi^{(0)}(1+h_\chi^{(1)});\; h_\varphi = h_\varphi^{(0)}(1+h_\varphi^{(1)}) \tag{A12b}$$

$$B = B_0(1+b^{(1)});\; B_\chi = B_\chi^{(0)}(1+b_\chi^{(1)}) \tag{A12c}$$

$$\nu_i = \nu_i^{(0)}(1+\nu_i^{(1)});\; \Omega_i = \Omega_i^{(0)}(1+\Omega_i^{(1)}) \tag{A12d}$$

where all the zeroth order quantities are functions of only ψ and the first order ones are of ψ and χ.

The plasma is assumed to have an axias of symmetry ($\partial A/\partial\varphi = 0$, where A is a scalar) More importantly, field lines are assumed to form nested flux surfaces. The symmetry provides an additional constant of motion and the field lines are called integrable. Even a small amount of perturbation can cause the surfaces to break and the field lines to wander chaotically in a volume instead of a surface in three dimensions [27].

High collisionality is taken into account as: $c_i/(qR\nu_i) \sim \mu$. The total plasma β is assumed to be low, since the Braginskii's stress tensors have been obtained by assuming a strong magnetic field.

A.5 Some key points

While performing ordering the following points should be taken into account [28].

1) Since $B_\varphi = \mu_0 I_T/(2\pi R)$ is created by the current, I_T, of the toroidal field coils:

$$\frac{1}{h_\psi}\frac{\partial B_\varphi}{\partial\psi} \sim \frac{\partial B_\varphi}{\partial r} \sim \frac{B_\varphi}{R}$$

2) Since B_χ is created by the plasma current density of the tokamak device, which changes radially by r:

$$\frac{1}{h_\psi}\frac{\partial B_\chi}{\partial\psi} \sim \frac{\partial B_\chi}{\partial r} \sim \frac{B_\chi}{r}$$

3) All the radial scale lengths, L_T, L_N, L_V, L_E, will be assumed to be at the same order, and:

$$\frac{1}{h_\psi}\frac{\partial T}{\partial\psi} \sim \frac{T}{L_T};\; \frac{1}{h_\psi}\frac{\partial N}{\partial\psi} \sim \frac{N}{L_T}$$

4) Since most of the quantities are assumed to have the following form: $F = F^{(n)}(\psi) + F^{(n+1)}(\psi,\chi)$; the derivation w.r.t. the χ will drop the order by one:

$$\frac{\partial F}{\partial\chi} \sim \frac{\partial F^{(n+1)}}{\partial\chi} \sim \mu\frac{\partial F^{(n)}}{\partial\chi}$$

5) Since $F(\psi,\chi)$ is assumed to have the form: $F(\psi,\chi)=\alpha\,\sin\chi+\beta\,\cos\chi$ the subsequent derivations will not change the order.

$$\frac{\partial^2 F}{\partial\chi^2}\sim\mu F$$

6) One exception is the parallel component of the heat flux vector.

$$q_{i,||}=-3.9\frac{P_i}{m_i\nu_i}\frac{1}{h_\chi}\frac{B_\chi}{B}\frac{\partial T_i}{\partial\chi}$$

Since

$$\frac{\partial}{\partial\chi}\ln\left(\frac{\partial T_i}{\partial\chi}\right)=\left(\frac{\partial T_i}{\partial\chi}\right)^{-1}\underbrace{\frac{\partial^2 T_i}{\partial\chi^2}}_{\sim\partial T_i/\partial\chi}\sim 1,$$

and

$$\frac{\partial\ln q_{i,||}}{\partial\chi}=\underbrace{\frac{\partial\ln P_i}{\partial\chi}}_{\sim\mu}-\underbrace{\frac{\partial\ln(m_i\nu_i)}{\partial\chi}}_{\sim\mu}-\underbrace{\frac{\partial\ln h_\chi}{\partial\chi}}_{\sim\mu}+\underbrace{\frac{\partial\ln(B_\chi/B)}{\partial\chi}}_{\sim\mu}+\underbrace{\frac{\partial}{\partial\chi}\ln\left(\frac{\partial T_i}{\partial\chi}\right)}_{\sim 1}\sim 1;$$

then

$$\frac{\partial\ln q_{i,||}}{\partial\chi}=\frac{1}{q_{i,||}}\frac{\partial q_{i,||}}{\partial\chi}\sim 1\;\Rightarrow\;\frac{\partial q_{i,||}}{\partial\chi}\sim q_{i,||}$$

7) How the ordering of the tensor terms is performed is explained with two examples:

7a) The first example will be a term including velocity gradient

$$\hat{b}\cdot\vec{\nabla}\vec{U}_i\cdot\hat{n}=\hat{b}\cdot\vec{\nabla}(\vec{U}_i\cdot\hat{n})-\hat{b}\cdot\vec{\nabla}\hat{n}\cdot(\hat{p}\,\vec{U}_i\cdot\hat{p}+\hat{b}\,\vec{U}_i\cdot\hat{b})$$

The first term is

$$\hat{b}\cdot\vec{\nabla}(\vec{U}_i\cdot\hat{n})=\underbrace{\frac{B_\varphi}{B}}_{\sim 1}\underbrace{\frac{1}{h_\chi}}_{\sim 1/r}\underbrace{\frac{\partial U_{||}}{\partial\chi}}_{\mu U_{||}}\sim\mu^2\frac{c_i}{r}\sim\mu\frac{c_i}{R}$$

The second term is

$$\hat{b}\cdot\vec{\nabla}\hat{n}\cdot\hat{p}\;\vec{U}_i\cdot\hat{p}=-\hat{n}\cdot\vec{\nabla}\hat{p}\cdot\hat{b}\,U_{i,\psi}=\underbrace{\frac{B_\varphi B_\chi}{B^2}}_{\sim\mu}\underbrace{\frac{1}{h_\psi}}_{\sim 1}\left(\underbrace{\frac{1}{h_\chi}}_{\sim 1/r}\underbrace{\frac{\partial h_\chi}{\partial\psi}}_{\sim 1}-\underbrace{\frac{1}{h_\varphi}}_{\sim 1/R}\underbrace{\frac{\partial h_\varphi}{\partial\psi}}_{\sim R}\right)\underbrace{U_{i,\psi}}_{\mu^6 c_i}\sim\mu^7\frac{c_i}{r}$$

And the last term is

$$\hat{b}\cdot\vec{\nabla}\hat{n}\cdot\hat{b}\;\vec{U}_i\cdot\hat{b}=-\hat{b}\cdot\vec{\nabla}\hat{b}\cdot\hat{n}\,U_{i,\beta}=\underbrace{\frac{B_\chi}{B}}_{\sim\mu}\underbrace{\frac{1}{h_\chi}}_{\sim 1/r}\underbrace{\frac{\partial\ln(Bh_\psi)}{\partial\chi}}_{\sim\mu}\underbrace{U_{i,\beta}}_{\mu^2 c_i}\sim\mu^4\frac{c_i}{r}\sim\mu^3\frac{c_i}{R}$$

7b) Another example will be a term including heat flux

$$\frac{2}{5P_i}\hat{b}\cdot\vec{\nabla}\vec{q}_i\cdot\hat{n}=\frac{2}{5P_i}\left[\hat{b}\cdot\vec{\nabla}(\vec{q}_i\cdot\hat{n})-\hat{b}\cdot\vec{\nabla}\hat{n}\cdot(\hat{p}\,\vec{q}\cdot\hat{p}+\hat{b}\,\vec{q}\cdot\hat{b})\right]$$

The first term is

$$\frac{2}{5P_i}\hat{b}\cdot\vec{\nabla}(\vec{q}_i\cdot\hat{n})=\frac{2}{5P_i}\underbrace{\frac{B_\varphi}{B}}_{\sim 1}\underbrace{\frac{1}{h_\chi}}_{\sim 1/r}\underbrace{\frac{\partial q_{||}}{\partial\chi}}_{q_{||}}\sim\frac{1}{P_i}\frac{1}{r}\frac{P_i}{R^2}\underbrace{\frac{T_i}{m_i\nu_i}}_{c_i^2/\nu_i}r\sim\frac{c_i}{R}\frac{c_i}{\nu_i R}\sim\mu\frac{c_i}{R}$$

The second term is

$$\frac{2}{5P_i}\hat{b}\cdot\vec{\nabla}\hat{n}\cdot\hat{p}\;\vec{q}_i\cdot\hat{p}=-\frac{2}{5P_i}\underbrace{\hat{n}\cdot\vec{\nabla}\hat{p}\cdot\hat{b}}_{\sim\mu/r}\,q_{i,\psi}\sim\frac{1}{P_i}\frac{\mu}{r}\frac{P_i}{R}\underbrace{\frac{T_i}{m_i\Omega_i}}_{a_i/c_i}\sim\underbrace{\frac{a_i}{R}}_{\sim\mu^4}\frac{c_i}{R}\sim\mu^4\frac{c_i}{r}$$

And the last term is

$$\frac{2}{5P_i}\hat{b}\cdot\vec{\nabla}\hat{n}\cdot\hat{b}\;\vec{q}_i\cdot\hat{b}=-\frac{2}{5P_i}\underbrace{\hat{b}\cdot\vec{\nabla}\hat{b}\cdot\hat{n}}_{\sim\mu^2/r}\,q_{i,\beta}\sim\frac{1}{P_i}\frac{\mu^2}{r}\frac{P_i}{L_T}\frac{T_i}{m_i\Omega_i}\sim\frac{a_i}{R}\frac{r}{L_T}\frac{c_i}{R}\sim\mu^3\frac{c_i}{R}$$

A.6 Toroidal momentum equation

In the (ψ,χ,φ) coordinate system, the toroidal component of the momentum equation is,

$$e_j N_j\hat{e}_\varphi\cdot(\vec{U}_j\times\vec{B})=e_j N_j U_\psi B_\chi=-\hat{e}_\varphi\cdot\left[\vec{\nabla}\cdot\vec{\Pi}_j+e_j N_j\vec{E}-\vec{R}_j-m_j N_j\frac{d\vec{U}_j}{dt}\right]\qquad\text{(A13)}$$

where the pressure gradient term has been dropped due to the toroidal axisymmetry, i.e.,

$$\hat{e}_\varphi\cdot\vec{\nabla}P_j=\frac{1}{h_\varphi}\frac{\partial P_j}{\partial\varphi}=0$$

Adding the equations for two species, ions (j = i) and electrons (j = e), one gets

$$B_\chi eN_i(U_{i,\psi}-U_{e,\psi})=B_\chi J_\psi=\hat{e}_\varphi\cdot\left[\vec{\nabla}\cdot\vec{\Pi}_i+m_i N_i\left(\frac{\partial}{\partial t}+\vec{U}_i\cdot\vec{\nabla}\right)\vec{U}_i\right],\qquad\text{(A14)}$$

where $e_i=e$, $e_e=-e$; $\vec{R}_i=\vec{R}$, $\vec{R}_e=-\vec{R}$, $m_i\gg m_e$; $\eta_i\gg\eta_e$ have been used. Applying the flux surface average operator, $\oint h_\varphi h_\chi(\cdot)d\varphi\,d\chi$, for both sides of this

equation

$$\oint h_\varphi h_\chi J_\psi\,d\chi=\oint J h_\varphi\,d\chi\;\hat{e}_\varphi\cdot\left[m_i N_i\left(\frac{\partial}{\partial t}+\vec{U}_i\cdot\vec{\nabla}\right)\vec{U}_i+\vec{\nabla}\cdot\vec{\Pi}_i\right]\qquad\text{(A15)}$$

where J is the jacobian and we have used the divergence-free magnetic field property, $\vec{\nabla}\cdot\vec{B}=0\;\Rightarrow\;h_\psi h_\varphi B_\chi=1$.

A.6.1 Contribution of the inertia terms

The time derivative term in the toroidal momentum equation is found as:

$$\oint J h_\varphi d\chi \left(m_i N_i \frac{\partial \vec{U}_i}{\partial t} \right) \cdot \hat{e}_\varphi = \oint J h_\varphi d\chi \left(m_i N_i \frac{\partial U_{\varphi,i}}{\partial t} \right) \tag{A16}$$

The rest of the inertia terms of the toroidal momentum equation is:

$$\begin{aligned} &\oint J h_\varphi d\chi m_i N_i \hat{e}_\varphi \cdot [(\vec{U}_i \cdot \vec{\nabla}) \vec{U}_i] \\ &= \oint J h_\varphi d\chi m_i N_i [\vec{U}_i \cdot \vec{\nabla} (\vec{U}_i \cdot \hat{e}_\varphi) - (\vec{U}_i \cdot \vec{\nabla} \hat{e}_\varphi) \cdot \vec{U}_i] \end{aligned} \tag{A17}$$

The first part of it can be written as:

$$\oint J h_\varphi d\chi m_i N_i [\vec{U}_i \cdot \vec{\nabla} (\vec{U}_i \cdot \hat{e}_\varphi)] = \oint J h_\varphi d\chi m_i N_i U_{\chi,i} \frac{1}{h_\chi} \frac{\partial U_{\varphi,i}}{\partial \chi} \tag{A17a}$$

Since,

$$\vec{U}_i \cdot \vec{\nabla} = \frac{U_{\psi,i}}{h_\psi} \frac{\partial}{\partial \psi} + \frac{U_{\chi,i}}{h_\chi} \frac{\partial}{\partial \chi} + \frac{U_{\varphi,i}}{h_\varphi} \frac{\partial}{\partial \varphi} \approx \frac{U_{\chi,i}}{h_\chi} \frac{\partial}{\partial \chi} + \frac{U_{\varphi,i}}{h_\varphi} \frac{\partial}{\partial \varphi}$$

$\vec{U}_i \cdot \hat{e}_\varphi = U_\varphi$, and $\partial U_{\varphi,i} / \partial \varphi = 0$ due to the toroidal axisymmetry.

By applying partial integration this term can be written as

$$\begin{aligned} &\oint J h_\varphi d\chi m_i N_i [\vec{U}_i \cdot \vec{\nabla} (\vec{U}_i \cdot \hat{e}_\varphi)] = -\oint d\chi U_{\varphi,i} m_i \frac{\partial}{\partial \chi} \left[\frac{J h_\varphi}{h_\chi} N_i U_{\chi,i} \right] \\ &= -\oint d\chi U_{\varphi,i} m_i \frac{\partial}{\partial \chi} \left[\frac{h_\varphi N_i U_{\chi,i}}{B_\chi} \right] = \oint d\chi U_{\varphi,i} m_i \left[J h_\varphi \frac{\partial N_i}{\partial t} - \frac{N_i U_{\chi,i}}{B_\chi} \frac{\partial h_\varphi}{\partial \chi} \right] \end{aligned} \tag{A17a'}$$

where the continuity equation has been used.

For the second part of equation (A17),

$$\begin{aligned} (\vec{U}_i \cdot \vec{\nabla} \hat{e}_\varphi) \cdot \vec{U}_i &= (\vec{U}_i \cdot \vec{\nabla} \hat{e}_\varphi) \cdot (U_\psi \hat{e}_\psi + U_\chi \hat{e}_\chi + U_\varphi \hat{e}_\varphi) \\ &\approx (\vec{U}_i \cdot \vec{\nabla} \hat{e}_\varphi) \cdot \hat{e}_\chi U_\chi = -U_\chi \frac{U_\varphi}{h_\chi} \frac{\partial \ln h_\varphi}{\partial \chi} \end{aligned} \tag{A17b}$$

where we used $\vec{U}_i \cdot \vec{\nabla} \hat{e}_\varphi \cdot \hat{e}_\varphi = (1/2) \vec{U}_i \cdot \vec{\nabla} (\hat{e}_\varphi \cdot \hat{e}_\varphi) = 0$ and the toroidal. symmetry.

Substituting into the integrand, we get

$$\begin{aligned} &\oint J h_\varphi d\chi m_i N_i [(\vec{U}_i \cdot \vec{\nabla} \hat{e}_\varphi) \cdot \vec{U}_i] = \oint d\chi U_{\varphi,i} m_i \left[\frac{J h_\varphi}{h_\chi} \frac{\partial \ln h_\varphi}{\partial \chi} N_i U_{\chi,i} \right] \\ &= \oint d\chi U_{\varphi,i} m_i \left[\frac{N_i U_{\chi,i}}{B_\chi} \frac{\partial h_\varphi}{\partial \chi} \right] \end{aligned} \tag{A18}$$

As a result the inertia term can be written as

$$\oint J h_\varphi \, d\chi \, \hat{e}_\varphi \cdot \left[m_i N_i \left(\frac{\partial}{\partial t} + \vec{U}_i \cdot \vec{\nabla} \right) \vec{U}_i \right] = \oint J h_\varphi \, d\chi \, m_i \frac{\partial (N_i U_{\varphi,i})}{\partial t} \tag{A19}$$

A.6.2 Contribution of the stress tensor

Toroidal component of the divergence of the symmetrical stress tensor is given as:

$$\hat{e}_\varphi \cdot (\vec{\nabla} \cdot \vec{\Pi}_i) = \frac{1}{h_\psi} \frac{\partial \Pi_{\psi\varphi}}{\partial \psi} + \frac{\Pi_{\psi\varphi}}{h_\psi} \frac{\partial \ln(h_\chi h_\varphi^2)}{\partial \psi} + \frac{1}{h_\chi} \frac{\partial \Pi_{\chi\varphi}}{\partial \chi} + \frac{\Pi_{\chi\varphi}}{h_\chi} \frac{\partial \ln(h_\psi h_\varphi^2)}{\partial \chi} \tag{A20}$$

Integration over the flux surface of this expression gives

$$\begin{aligned} \oint J h_\varphi \, d\chi \, \hat{e}_\varphi \cdot (\vec{\nabla} \cdot \vec{\Pi}_i) &= \oint d\chi \left[\frac{\partial (h_\chi h_\varphi^2 \Pi_{\psi\varphi})}{\partial \psi} + \frac{\partial (h_\psi h_\varphi^2 \Pi_{\chi\varphi})}{\partial \chi} \right] \\ &= \frac{\partial}{\partial \psi} \oint h_\chi h_\varphi^2 \Pi_{\psi\varphi} \, d\chi \end{aligned} \tag{A21}$$

Only the (ψ, φ) components of the stress tensor will contribute to the toroidal momentum equation. (ψ, φ) component of the stress tensor can be found by following calculation:

$$\Pi_{\psi\varphi} = -\frac{B_\chi}{B} \Pi_{pb} + \frac{B_\varphi}{B} \Pi_{pn} \tag{A22}$$

i) Since the **parallel viscosity tensor** has only the diagonal terms, it will not contribute to this equation.

ii) The contribution from the **perpendicular stress tensor** is found as:

$$\begin{aligned} (\Pi_{1,2,i})_{\psi\varphi} = -\eta_{1,i} \Bigg\{ & -\frac{B_\chi}{B} \left[(\hat{p} \cdot \vec{\nabla} \vec{U}_i \cdot \hat{b} + \hat{b} \cdot \vec{\nabla} \vec{U}_i \cdot \hat{p}) + \frac{2}{5 P_i} (\hat{p} \cdot \vec{\nabla} \vec{q}_i \cdot \hat{b} + \hat{b} \cdot \vec{\nabla} \vec{q}_i \cdot \hat{p}) \right] \\ & + 4 \frac{B_\varphi}{B} \left[(\hat{p} \cdot \vec{\nabla} \vec{U}_i \cdot \hat{n} + \hat{n} \cdot \vec{\nabla} \vec{U}_i \cdot \hat{p}) + \frac{2}{5 P_i} (\hat{p} \cdot \vec{\nabla} \vec{q}_i \cdot \hat{n} + \hat{n} \cdot \vec{\nabla} \vec{q}_i \cdot \hat{p}) \right] \end{aligned} \tag{A23a}$$

After ordering, the contribution from the velocity gradient terms can be found as:

$$-4 \eta_{1,i} \frac{B_\varphi}{B} \hat{p} \cdot \vec{\nabla} U_{i,\|} \tag{A23a'}$$

As compared to this term, the contribution from the heat flux gradient terms has been found negligible. The contribution of the perpendicular stress tensor to the toroidal momentum equation is

$$-\frac{12}{10} \frac{m_i}{e_i} \frac{\partial}{\partial \psi} \left\{ h_\varphi^2 B_\varphi^2 \oint d\chi \frac{1}{\Omega_i \nu_i} \frac{B_\chi}{B_\varphi} \frac{J}{B^2} \frac{P_i}{h_\psi} \frac{1}{\partial \psi} \frac{\partial U_{i,\|}}{\partial \psi} \right\} \tag{A23a''}$$

where the explicit definition of $\eta_{3,i}$ and Ampere's Law at the leading order $\partial(h_\varphi B_\varphi)/\partial\chi = 0$ [6] has been used.

iii) And the contribution from the **gyro-stress tensor** is found as:

$$(\Pi_{3,4,i})_{\psi\varphi}=\eta_{3,i}\left\{-\frac{B_\chi}{B}\left[(\hat{p}\cdot\vec{\nabla}\vec{U}_i\cdot\hat{p}-\hat{b}\cdot\vec{\nabla}\vec{U}_i\cdot\hat{b})+\frac{2}{5P_i}(\hat{p}\cdot\vec{\nabla}\vec{q}_i\cdot\hat{p}-\hat{b}\cdot\vec{\nabla}\vec{q}_i\cdot\hat{b})\right]\right.$$
$$\left.-2\frac{B_\varphi}{B}\left[(\hat{b}\cdot\vec{\nabla}\vec{U}_i\cdot\hat{n}+\hat{n}\cdot\vec{\nabla}\vec{U}_i\cdot\hat{b})+\frac{2}{5P_i}(\hat{b}\cdot\vec{\nabla}\vec{q}_i\cdot\hat{n}+\hat{n}\cdot\vec{\nabla}\vec{q}_i\cdot\hat{b})\right]\right. \tag{A23b}$$

After ordering, the contribution from the velocity gradient terms are found as:

$$-2\eta_{3,i}\frac{B_\varphi}{B}[\hat{b}\cdot\vec{\nabla}U_{i,\|}-\hat{n}\cdot\vec{\nabla}\hat{b}\cdot\hat{n}U_{i,\|}]=-2\eta_{3,i}\frac{B_\varphi^2}{h_\chi B^3}\frac{\partial(BU_{i,\|})}{\partial\chi} \tag{A23b'}$$

And the contribution from the heat flux gradient terms can be found as:

$$-2\eta_{3,i}\frac{B_\varphi}{B}\frac{2}{5P_i}[\hat{b}\cdot\vec{\nabla}q_{i,\|}-\hat{n}\cdot\vec{\nabla}\hat{b}\cdot\hat{n}q_{i,\|}]=-2\eta_{3,i}\frac{B_\varphi^2}{h_\chi B^3}\frac{\partial(Bq_{i,\|})}{\partial\chi} \tag{A23b''}$$

These two contributions may be combined as

$$\frac{m_i}{e_i}\frac{\partial}{\partial\psi}\left\{h_\varphi^2B_\varphi^2\oint d\chi\left[\frac{P_i}{B^4}\frac{\partial(U_{i,\|}B)}{\partial\chi}+\frac{8}{5}\frac{q_{i,\|}}{B^4}\frac{\partial B}{\partial\chi}\right]\right\} \tag{A23b'''}$$

where the explicit definition of $\eta_{3,i}$, partial integration and Ampere Law at the leading order $\partial(h_\varphi B_\varphi)/\partial\chi=0$ [6] has been used.

A.6.3 Toroidal momentum equation for arbitrary and circular cross section tokamaks

By combining these effects and expanding them, one gets the toroidal momentum equation for large aspect ratio tokamak with arbitrary cross section:

$$2\pi m_i N_i J h_\varphi\frac{\partial U_{\varphi,i}}{\partial t}-\oint h_\varphi h_\chi J_\psi d\chi$$
$$=\frac{m_i h_\varphi^2}{e_i}\frac{\partial}{\partial\psi}\left[-0.4P_i\frac{U_{\chi,i}}{B_\chi}\oint b^{(1)}\frac{\partial n^{(1)}}{\partial\chi}d\chi+1.2(2\pi)P_i\frac{\nu_i}{\Omega_i}\frac{h_\chi}{h_\psi B}\frac{\partial U_{\varphi,i}}{\partial\psi}\right] \tag{A24}$$

Claassen and Gerhauser [7] have already obtained the toroidal momentum transport equation for tokamak plasmas with circular cross section.

$$m_i N_i\frac{\partial U_{\varphi,i}}{\partial t}=\frac{\partial}{\partial r}\left[\eta_{2,i}\left(\frac{\partial U_{\varphi,i}}{\partial r}-\frac{0.107q^2}{1+Q^2/S^2}\frac{\partial\ln T_i}{\partial r}\frac{B_\varphi}{B_\theta}U_{\theta,i}\right)\right]+J_r B_\theta \tag{A25}$$

The quantities Q and S are obtained from various drifts and dissipation processes [6].

$$Q=4\frac{B_\varphi}{B}U_{\theta,i}-\frac{5}{2}\frac{T_i}{e_i B}\frac{\partial\ln N_i^2T_i}{\partial r} \tag{A25a}$$

$$S=\frac{2r\chi_{\|,i}}{q^2R^2N_i} \tag{A25b}$$

where $\chi_{\|,i}=3.9P_i/m_i\nu_i$, is the parallel ion heat diffusion coefficient.

The effects of the charge exchange and the momentum injection may be included into the equation by changing the time derivative:

$$\frac{\partial U_{\varphi,i}}{\partial t} \rightarrow \left(\frac{\partial}{\partial t} + \nu_{cx} \right) U_{\varphi,i} - \dot{m}_{\varphi,i} \tag{A26}$$

A.7 Parallel momentum equation

The momentum equations for species, j = i and j = e, are written as follows:

$$m_i N_i \frac{d\vec{U}_i}{dt} = -\vec{\nabla} P_i - \vec{\nabla} \cdot \vec{\vec{\Pi}}_i + eN(\vec{E} + \vec{U}_i \times \vec{B}) + \vec{R} \tag{A27a}$$

$$m_e N_e \frac{d\vec{U}_e}{dt} = -\vec{\nabla} P_e - \vec{\nabla} \cdot \vec{\vec{\Pi}}_e - eN(\vec{E} + \vec{U}_e \times \vec{B}) - \vec{R} \tag{A27b}$$

By adding these two equations, one gets

$$m_i N_i \left(\frac{\partial \vec{U}_i}{\partial t} + \vec{U}_i \cdot \vec{\nabla} \vec{U}_i \right) + \vec{\nabla} P + \vec{\nabla} \cdot \vec{\vec{\Pi}}_i + eN(\vec{U}_i - \vec{U}_e) \times \vec{B} = 0 \tag{A28}$$

where $e_i = e$, $e_e = -e$; $\vec{R}_i = \vec{R}$, $\vec{R}_e = -\vec{R}$, $m_i \gg m_e$; $\eta_i \gg \eta_e$; $P = P_i + P_e$ have been used.

The JB, $(B = |\vec{B}|)$ weighted parallel component of this result will be integrated along χ in order to remove χ dependency. The term including the magnetic field will be dropped since $\hat{n} \parallel \vec{B}$ and

$$\hat{n} \cdot [(\vec{U}_i - \vec{U}_e) \times \vec{B}] = 0.$$

The pressure term will also be dropped due to the weighting function JB as follows:

$$\begin{aligned} \oint JB\hat{n} \cdot \vec{\nabla} P \, d\chi &= \oint JB \frac{B_\chi}{B} \frac{1}{h_\chi} \frac{\partial P}{\partial \chi} d\chi \\ &= \oint h_\psi h_\varphi B_\chi \frac{\partial P}{\partial \chi} d\chi = -\oint P \frac{\partial (h_\psi h_\varphi B_\chi)}{\partial \chi} d\chi = 0 \end{aligned}$$

where the axial symmetry and $\partial_\chi (h_\psi h_\varphi B_\chi) = 0$, a property of the divergence-free magnetic field, was used., since we get

$$\vec{\nabla} \cdot \vec{B} = \vec{\nabla} \cdot (B_\chi \hat{e}_\chi + B_\varphi \hat{e}_\varphi) = \frac{1}{J} \frac{\partial (h_\psi h_\varphi B_\chi)}{\partial \chi} = 0$$

Hence, one obtains

$$\oint JB \left[m_i N_i \left(\frac{\partial \vec{U}_i}{\partial t} + \vec{U}_i \cdot \vec{\nabla} \vec{U}_i \right) + \vec{\nabla} \cdot \vec{\vec{\Pi}}_i \right] \cdot \hat{n} \, d\chi = 0 \tag{A29}$$

A.7.1 Contribution of the inertia terms

The contribution of the inertia term can be put into the following form [8]

$$\oint JB\left[m_i N_i\left(\frac{\partial \vec{U}_i}{\partial t}+\vec{U}_i\cdot\vec{\nabla}\vec{U}_i\right)\right]\cdot\hat{n}\,d\chi=\oint JB\,m_i N_i\frac{\partial U_{\parallel,i}}{\partial t}d\chi$$
$$+\oint m_i N_i\frac{B}{B_\chi}\left[U_{\chi,i}\frac{\partial U_{\parallel,i}}{\partial\chi}+U_{\beta,i}^2\frac{B_\chi}{B}\frac{\partial\ln Bh_\psi}{\partial\chi}-U_{\parallel,i}U_{\beta,i}\frac{B_\varphi}{B}\frac{\partial\ln B}{\partial\chi}\right]d\chi \tag{A30}$$

By applying the ordering scheme of regular perturbation given in the previous sub-chapter, the equation (A30) becomes as follows:

$$\oint JB\,m_i N_i\left(\frac{\partial\vec{U}_i}{\partial t}+\vec{U}_i\cdot\vec{\nabla}\vec{U}_i\right)\cdot\hat{n}\,d\chi=m_i N_i\oint JB\frac{\partial U_{\parallel,i}}{\partial t}d\chi$$
$$-m_i N_i\left\{U_{\varphi,i}^2-2\frac{B_\chi U_{\varphi,i}-B_\varphi U_{\chi,i}}{B_\chi^2}\left[B_\varphi U_{\chi,i}-\frac{T_i}{e_i}\frac{\partial\ln T_i N_i^2}{h_\psi\,\partial\psi}\right]\right\}\oint b^{(1)}\frac{\partial n^{(1)}}{\partial\chi}d\chi \tag{A30a}$$

For the details of the decomposition of the parallel velocity into the poloidal and the toroidal components see Appendix B of this report.

A.7.2 Contribution of the stress tensor

By considering the symmetry of the stress tensor, i.e., $\vec{\vec{\Pi}}=\vec{\alpha}\vec{\beta}+\vec{\beta}\vec{\alpha}$, the term including the stress tensor in the equation (A29) can be transformed into the following form:

$$\oint JB(\vec{\nabla}\cdot\vec{\vec{\Pi}}_i)\cdot\hat{n}\,d\chi=\frac{\partial}{\partial\psi}\oint\frac{JB}{h_\psi}\Pi_{\psi\parallel}\,d\chi-\oint J\left(\Pi_{\psi\parallel}\frac{1}{h_\psi}\frac{\partial B}{\partial\psi}+\Pi_{\chi\parallel}\frac{1}{h_\chi}\frac{\partial B}{\partial\chi}\right)d\chi$$
$$-\oint JB[\hat{p}\cdot\vec{\nabla}\hat{n}\cdot\hat{p}\Pi_{\psi\psi}+\hat{p}\cdot\vec{\nabla}\hat{n}\cdot\hat{b}\Pi_{\psi\beta}+\hat{b}\cdot\vec{\nabla}\hat{n}\cdot\hat{p}\Pi_{\beta\psi}$$
$$+\hat{b}\cdot\vec{\nabla}\hat{n}\cdot\hat{b}\Pi_{\beta\beta}+\hat{n}\cdot\vec{\nabla}\hat{n}\cdot\hat{p}\Pi_{\parallel\psi}+\hat{n}\cdot\vec{\nabla}\hat{n}\cdot\hat{b}\Pi_{\parallel\beta}] \tag{A31}$$

where $\Pi_{\psi\parallel}$, $\Pi_{\chi\parallel}$, $\Pi_{\psi\psi}$, $\Pi_{\psi\beta}$, $\Pi_{\beta\psi}$, $\Pi_{\beta\beta}$, $\Pi_{\parallel\psi}$, $\Pi_{\parallel\beta}$ terms are the $\hat{p}\hat{n}$, $\hat{e}_\chi\hat{n}$ $\hat{p}\hat{p}$, $\hat{p}\hat{b}$, $\hat{b}\hat{p}$, $\hat{b}\hat{b}$, $\hat{n}\hat{p}$, $\hat{n}\hat{b}$ components of the stress tensor, respectively. For example, $\Pi_{\beta\psi}=\hat{b}\cdot\vec{\vec{\Pi}}\cdot\hat{p}$. The Christoffel symbols in the general orthogonal toroidal coordinate system may be found in Appendix A of Ref. [29].

i) Parallel stress tensor,

$$\oint JB\vec{\nabla}\cdot\vec{\vec{\Pi}}_{0,i}\cdot\hat{n}\,d\chi=\frac{3\eta_{0,i}}{h_\chi}\left[U_{\chi,i}+\frac{1.83}{e_i B_\varphi}\frac{\partial T_i}{h_\psi\,\partial\psi}\right]\oint\left(\frac{\partial b^{(1)}}{\partial\chi}\right)^2 d\chi$$
$$-0.123\,m_i N_i\frac{B_\varphi^2}{B_\chi^2}\left[3.69\,U_{\chi,i}-1.56\frac{T_i}{e_i B_\varphi}\frac{\partial\ln N_i^2}{h_\psi\,\partial\psi}\right]$$
$$\times\left[4U_{\chi,i}-2.5\frac{T_i}{e_i B_\varphi}\frac{\partial\ln N_i^2 T_i}{h_\psi\,\partial\psi}\right]\oint b^{(1)}\frac{\partial n^{(1)}}{\partial\chi}d\chi \tag{A31a}$$

where $\partial t_i^{(1)}/\partial\chi=-2\partial n_i^{(1)}/\partial\chi$ has been used [6].

ii) Perpendicular stress tensor,

$$\oint JB\vec{\nabla}\cdot(\vec{\vec{\Pi}}_{1,i}+\vec{\vec{\Pi}}_{2,i})\cdot\hat{n}\,d\chi=-2\pi h_\varphi B_\varphi\frac{\partial}{\partial\psi}\left(\eta_{2,i}\frac{h_\chi}{h_\psi}\frac{\partial U_{\varphi,i}}{\partial\psi}\right) \tag{A31b}$$

iii) Gyro-stress tensor,

$$\begin{aligned}\oint JB\vec{\nabla}\cdot(\vec{\vec{\Pi}}_{3,i}+\vec{\vec{\Pi}}_{4,i})\cdot\hat{n}\,d\chi &= 0.4\frac{m_i}{e_i}h_\varphi B_\varphi\frac{\partial}{\partial\psi}\left[\frac{P_i}{B_\chi}U_{\chi,i}\oint b^{(1)}\frac{\partial n^{(1)}}{\partial\chi}d\chi\right]\\ &-2\frac{m_i}{e_i}h_\varphi B_\varphi\left\{\frac{P_i}{B_\varphi}\frac{\partial U_{\varphi,i}}{\partial\psi}+\frac{1}{B_\chi}\frac{\partial P_i}{\partial\psi}\left[\frac{T_i}{e_iB_\varphi}\frac{\partial\ln T_iN_i^2}{h_\psi\partial\psi}-U_{\chi,i}\right]\right\}\oint b^{(1)}\frac{\partial n^{(1)}}{\partial\chi}d\chi\end{aligned} \tag{A31c}$$

A.7.3 Parallel momentum equation for arbitrary and circular cross section tokamaks

The contributions from the inertia and stress tensor terms can be combined as [8],

$$\begin{aligned}&\oint JB\left[m_iN_i\left(\frac{\partial\vec{U}_i}{\partial t}+\vec{U}_i\cdot\vec{\nabla}\vec{U}_i\right)+\vec{\nabla}\cdot\vec{\vec{\Pi}}_i\right]\cdot\hat{n}\,d\chi\\ &=(1+2q^2)B_\chi\frac{\partial U_\chi}{\partial t}+\frac{3\eta_{0,i}}{h_\chi}\left[U_{\chi,i}+\frac{1.83}{e_iB_\varphi}\frac{1}{h_\psi}\frac{\partial T_i}{\partial\psi}\right]\oint\left(\frac{\partial b^{(1)}}{\partial\chi}\right)^2d\chi\\ &-2m_iN_i\left\{\frac{T_i}{e_iB_\chi}\frac{1}{h_\psi}\frac{\partial U_{\varphi,i}}{\partial\psi}+\frac{1}{2}U_{\varphi,i}^2-\frac{B_\varphi}{B_\chi}U_{\varphi,i}\left[U_{\chi,i}-\frac{T_i}{e_iB_\varphi}\frac{1}{h_\psi}\frac{\partial\ln N_i^2T_i}{\partial\psi}\right]\right.\\ &\left.+1.90\left(\frac{B_\varphi}{B_\chi}\right)^2\left[U_{\chi,i}-0.8\frac{T_i}{e_iB_\varphi}\frac{1}{h_\psi}\frac{\partial\ln N_i^{1.6}T_i}{\partial\psi}\right]^2\right\}\oint b^{(1)}\frac{\partial n^{(1)}}{\partial\chi}d\chi=0\end{aligned} \tag{A32}$$

where the term with the the time derivative of the toroidal velocity in the inertia contribution and the $\eta_{2,i}$ term in the perpendicular stress tensor contribution have eliminated each other in view of the equation (A24).

The equation (A32) is valid for large aspect ratio tokamaks with arbitrary cross-section. In order to obtain the parallel momentum equation for tokamaks with circular cross-section, the magnetic field will be taken as $B=B_0(1+\varepsilon\cos\chi)^{-1}$, where B_0 is the value of the magnetic field at the magnetic axis. The perturbation terms of the magnetic field and the density are given as follows [6],

$$b^{(1)}=-\cos\chi, \tag{A33}$$

$$n^{(1)}=n^{(1)}_{\cos}\cos\chi+n^{(1)}_{\sin}\sin\chi \tag{A34}$$

where the coefficients are given [6] as

$$n^{(1)}_{\cos}=\frac{5\varepsilon Q}{Q^2+S^2}\frac{1}{e_i\,B_\varphi\,h_\psi}\frac{\partial T_i}{\partial\psi}, \tag{A34a}$$

$$n^{(1)}_{\sin}=\frac{-5\varepsilon S}{Q^2+S^2}\frac{1}{e_i\,B_\varphi\,h_\psi}\frac{\partial T_i}{\partial\psi} \tag{A34b}$$

here Q and S are given in equations (A25a) and (A25b). By changing ψ and χ with r and θ, taking $h_r = 1;\ h_\theta = r$ and evaluating the integrals in the equation (A32), the parallel momentum equation for large aspect ratio tokamaks with circular cross sections becomes [8]:

$$
\begin{aligned}
m_i N_i (1+2q^2)\frac{B_\theta^{(0)}}{B_\varphi^{(0)}}\frac{\partial U_{\theta,i}^{(2)}}{\partial t} = &-\frac{3\eta_{0,i}}{2R^2}\left(U_{\theta,i}^{(2)} + \frac{1.833}{e_i B_\varphi}\frac{\partial T_i}{\partial r}\right) \\
&+ 0.54\frac{\eta_{2,i}}{1+Q^2/S^2} q^2 \frac{e_i B_\varphi}{T_i}\frac{\partial \ln T_i}{\partial r}\left[\frac{T_i}{e_i B_\theta}\frac{\partial U_{\varphi,i}^{(1)}}{\partial r} + \frac{1}{2} U_{\varphi,i}^{(1)\,2}\right. \\
&\left. - U_{\varphi,i}^{(1)}\frac{B_\varphi}{B_\theta}\left(U_{\theta,i}^{(2)} - \frac{T_i}{e_i B_\varphi}\frac{\partial \ln N_i^2 T_i}{\partial r}\right) + 1.90\frac{B_\varphi^2}{B_\theta^2}\left(U_{\theta,i}^{(2)} - 0.8\frac{T_i}{e_i B_\varphi}\frac{\partial \ln N_i^{1.6} T_i}{\partial r}\right)^2\right] \\
&- J_r B_\varphi
\end{aligned}
\qquad \text{(A35)}
$$

Appendix B. Decomposition and Average of the Parallel Velocity

In this appendix we will first show that, for the subsonic speeds, the velocity vector can be written in a special form (equation (B17)) by following the procedure described in Ref. [10, 11] then based on this form, the flux surface average of the parallel velocity will be calculated.

B.1 Flux surface average

The flux surface average of a quantity A is usually defined [11] as

$$<A>\equiv\frac{\oint\frac{d\theta}{\vec{B}\cdot\vec{\nabla}\theta}A}{\oint\frac{d\theta}{\vec{B}\cdot\vec{\nabla}\theta}} \tag{B1}$$

where $\vec{\nabla}\theta=h_\theta^{-1}\hat{e}_\theta$, and $\vec{B}\cdot\vec{\nabla}\theta=h_\theta^{-1}B_\theta$. Since $\vec{\nabla}\cdot\vec{B}=0$, $h_r h_\varphi B_\theta=1$ and therefore $\vec{B}\cdot\vec{\nabla}\theta=(h_r h_\theta h_\varphi)^{-1}=J^{-1}$. The flux surface average can be related to the above definition as in [6]

$$<A>\equiv\frac{\oint AJd\theta}{\oint Jd\theta} \tag{B2}$$

In the standard toroidal geometry, h_r=1, h_θ=r and h_φ=R. Therefore, in this geometry, the flux surface average will be following

$$<A>\equiv\frac{\oint d\theta\, r R_0(1+\frac{r}{R_0}\cos\theta)A}{\oint d\theta\, r R_0(1+\frac{r}{R_0}\cos\theta)}=\oint\frac{d\theta}{2\pi}(1+\frac{r}{R_0}\cos\theta)A \tag{B3}$$

where the term including cosθ in the denominator of the above equation has vanished due to the 2π periodicity of the function cosine.

B.2 Decomposition of the parallel velocity

By neglecting the time variation of the density, the continuity equation will take the following form

$$\vec{\nabla}\cdot\vec{\Gamma}_i=0 \tag{B4}$$

where $\vec{\Gamma}_i=N_i\vec{U}_i$. Using the axisymmetry (∂_φ=0) and neglecting the radial velocity contribution at the leading order, the equation (B4) will be

$$\frac{\partial}{\partial\chi}\left(h_\psi h_\varphi \Gamma_{\chi i}\right)=0 \tag{B5}$$

This result implies that $h_\psi h_\varphi \Gamma_{\chi i}$ can be a function of ψ only. As a result of the $\vec{\nabla}\cdot\vec{B}=0$, the scale factor in the ψ direction will be $h_\psi=(h_\phi B_\chi)^{-1}$.

$$N_i = N_i^{(0)}(\psi) + N_i^{(1)}(\psi,\chi)$$

and

$$U_{i\chi} = U_{i\chi}^{(2)}(\psi) + U_{i\chi}^{(3)}(\psi,\chi)$$

Therefore, at the leading order,

$$\Gamma_{\chi i} = N_i^{(0)}(\psi)\, U_{\chi i}^{(2)}(\psi) \tag{B6}$$

Hence,

$$h_\psi h_\varphi \Gamma_{\chi i} = \frac{N_i^{(0)} U_{\chi i}^{(2)}}{B_\chi} = N_i^{(0)}(\psi)\frac{\vec{U}_i \cdot \vec{B}_\chi}{B_\chi^2}$$

and,

$$\frac{\vec{U}_i \cdot \vec{B}_\chi}{B_\chi^2} \equiv K(\psi) \tag{B7}$$

The velocity vector can be decomposed as

$$\vec{U}_i = \hat{n}\, U_{i\|} + \vec{U}_{i\perp} \tag{B8}$$

The scalar product of the equation (B8) and the poloidal magnetic field, $\vec{B}_\chi$, is

$$\vec{U}_i \cdot \vec{B}_\chi = \vec{B}_\chi \cdot \hat{n}\, U_{i\|} + \vec{B}_\chi \cdot \vec{U}_{i\perp} \tag{B9}$$

where

$$\vec{B}_\chi \cdot \hat{n} = \vec{B}_\chi \cdot \vec{B}/B = B_\chi^2/B$$

Dividing the equation (B9) by B_χ^2/B, one finds

$$\left(\frac{\vec{U}_i \cdot \vec{B}_\chi}{B_\chi^2}\right) B = U_{i\|} + \frac{\vec{B}_\chi \cdot \vec{U}_{i\perp}}{B_\chi^2} B \tag{B10}$$

And considering the equation (B7), we find for $U_{||}$,

$$U_{i\|} = K(\psi) B - \frac{\vec{B}_\chi \cdot \vec{U}_{i\perp}}{B_\chi^2} B \tag{B11}$$

Substituting $U_{\|}$ into the equation (B8),

$$\vec{U}_i = \vec{U}_{i\perp} + K(\psi)\vec{B} - \frac{\hat{e}_\chi \cdot \vec{U}_{i\perp}}{B_\chi}\vec{B} \tag{B12}$$

is found, where $\hat{e}_\chi = \vec{B}_\chi / B_\chi$.

$$\vec{U}_i = \left[(\hat{e}_\chi \hat{e}_\chi + \hat{e}_\varphi \hat{e}_\varphi) - \frac{\vec{B}_\chi + \vec{B}_\varphi}{B_\chi}\hat{e}_\chi \right] \cdot \vec{U}_{i\perp} + K(\psi)\vec{B} \tag{B13}$$

and hence

$$\vec{U}_i = \hat{e}_\varphi \left(\hat{e}_\varphi - \frac{B_\varphi}{B_\chi} \hat{e}_\chi \right) \cdot \vec{U}_{i\perp} + K(\psi)\vec{B} \qquad \text{(B14)}$$

Since

$$\hat{e}_\varphi - \frac{B_\varphi}{B_\chi}\hat{e}_\chi = -\frac{B}{B_\chi}\hat{b}$$

and

$$U_{i\perp} = \hat{b}\cdot\vec{U}_{i\perp}$$

for the velocity vector, we find

$$\vec{U}_i = -U_{i\perp}\frac{B}{B_\chi}\hat{e}_\varphi + K(\psi)\vec{B} \qquad \text{(B15)}$$

By following the scaling relationships in the Appendix A, the radial momentum equation can reduced to the following form as in the Ref. [6]

$$e_i B N_i^{(0)}(\psi)\hat{b}\cdot\vec{U}_i = e_i B N_i^{(0)}(\psi) U_{i\perp} = -\hat{p}\cdot[\vec{\nabla} P_i^{(0)} + e_i N_i^{(0)}\vec{\nabla} V] + O(\mu^3) \qquad \text{(B16)}$$

Here $[\vec{\nabla} P_i^{(0)} + e_i N_i^{(0)}\vec{\nabla} V]$ is the function of ψ only. In the standard geometry the magnetic field B, can be written as $B=B_0(\psi)/h$, where $h=R/R_0$. With this form of the magnetic field, $BU_{i\perp}$ is found to be the function of ψ as implied by the equation (B16). Hence, defining a function $G(\psi)$, the velocity vector can be written as

$$\vec{U}_i = K(\psi)\vec{B} + G(\psi)R\,\hat{e}_\varphi \qquad \text{(B17)}$$

where $R=R_0+r\cos\theta$ is the major radius, and r is the minor radius.

B.3 Averaging the parallel velocity

The form given in equation (B17) is valid for the subsonic speeds, i.e., incompressible fluid and the function $K(\psi)$ is proportional to the poloidal velocity, while $G(\psi)$ is proportional to the perpendicular velocity [11]. This equation can be written as

$$\vec{U}_i = KB_\chi\hat{e}_\chi + (KB_\varphi + GR)\hat{e}_\varphi \qquad \text{(B18)}$$

Based on this equation, parallel velocity is found as

$$BU_{i\|} = KB_\chi^2 + KB_\varphi^2 + GRB_\varphi \qquad \text{(B19)}$$

Flux surface average of the equation (B19) is

$$\langle BU_{i\|}\rangle = K\langle B_\chi^2\rangle + K\langle B_\varphi^2\rangle + G\langle RB_\varphi\rangle \qquad \text{(B20)}$$

And the toroidal velocity is

$$RU_{i\varphi} = KRB_\varphi + GR^2 \qquad \text{(B21)}$$

The average of the equation (B21) is

$$\langle RU_{i\varphi}\rangle = K\langle RB_\varphi\rangle + G\langle R^2\rangle \qquad \text{(B22)}$$

Substituting G obtained from the equation (B22) into the (B20), we get

$$<BU_{\|}>=<B_\chi^2>(1+2q^2)K+\frac{R_0 B_\varphi^{(0)}}{<R^2>}<RU_\varphi> \tag{B23}$$

where

$$q^2=\frac{(R_0 B_\varphi^{(0)})^2}{2<B_\chi^2>}(<R^{-2}>-<R^2>^{-1}) \tag{B24}$$

and $K(\psi)\equiv\vec{U}_i\cdot\vec{B}_\chi/B_\chi^2$ (as defined in equation (B7)).

In the large aspect ratio circular limit, q reduces to the usual safety factor [11] as follows: At the leading order, $B_\varphi^{(0)}=B_0$ and the poloidal magnetic field is given as

$$B_\theta=\frac{rB_0}{q_s R} \tag{B25}$$

where q_s is the usual safety factor. Average of R^{-2} is calculated as follows:

$$\begin{aligned}
<R^{-2}>&=R_0^{-2}<\left(1+\frac{r}{R_0}\cos\theta\right)^{-2}>=R_0^{-2}\oint\frac{d\theta}{2\pi}\left(1+\frac{r}{R_0}\cos\theta\right)^{-1}\\
&=R_0^{-2}\oint\frac{d\theta}{2\pi}\left(1-\frac{r}{R_0}\cos\theta+\frac{r^2}{R_0^2}\cos^2\theta+\cdots\right)\\
&\cong R_0^{-2}\oint\frac{d\theta}{2\pi}\left(1+\frac{r^2}{R_0^2}\cos^2\theta\right)^{-1}=R_0^{-2}\left(1+\frac{r^2}{R_0^2}\right)
\end{aligned}$$

Average of R^2 is:

$$\begin{aligned}
<R^2>&=R_0^2<\left(1+\frac{r}{R_0}\cos\theta\right)^2>=R_0^2\oint\frac{d\theta}{2\pi}\left(1+\frac{r}{R_0}\cos\theta\right)^3\\
&=R_0^2\oint\frac{d\theta}{2\pi}\left(1+\frac{r}{R_0}\cos\theta+3\frac{r^2}{R_0^2}\cos^2\theta+\cdots\right)\\
&\cong R_0^2\oint\frac{d\theta}{2\pi}\left(1+3\frac{r^2}{R_0^2}\cos^2\theta\right)=R_0^2\left(1+\frac{3}{2}\frac{r^2}{R_0^2}\right)
\end{aligned}$$

Lastly, the average of the square of the poloidal magnetic field is:

$$<B_\theta^2>=<\frac{r^2B_0^2}{q_s^2R^2}>=\frac{r^2B_0^2}{q_s^2}<R^{-2}>=\frac{r^2B_0^2}{q_s^2}R_0^{-2}\left(1+\frac{1}{2}\frac{r^2}{R_0^2}\right)$$

Substituting these averages in the equation (B24), one gets the usual safety factor q_s

$$q^2=\frac{R_0^2B_0^2}{2\frac{r^2B_0^2}{q_s^2R_0^2}\left(1+\frac{1}{2}\frac{r^2}{R_0^2}\right)}\left[R_0^{-2}\left(1+\frac{1}{2}\frac{r^2}{R_0^2}\right)-R_0^{-2}\left(1+\frac{3}{2}\frac{r^2}{R_0^2}\right)^{-1}\right]$$

$$=\frac{1}{2}q_s^2\frac{R_0^2}{r^2}\left(1-\frac{1}{\left(1+\frac{1}{2}\frac{r^2}{R_0^2}\right)\left(1+\frac{3}{2}\frac{r^2}{R_0^2}\right)}\right)=\frac{1}{2}q_s^2\frac{R_0^2}{r^2}\left[1-\frac{1}{1+\frac{1}{2}\frac{r^2}{R_0^2}+\frac{3}{2}\frac{r^2}{R_0^2}+\cdots}\right]$$

$$=\frac{1}{2}q_s^2\frac{R_0^2}{r^2}\left[1-\left(1+2\frac{r^2}{R_0^2}\right)\right]=q_s^2$$

In the standard geometry the equation (B23) will be reduced to the following form:

$$<BU_{\parallel}>=B_\theta^{(0)^2}(1+2q^2)K+B_\varphi^{(0)}U_\varphi^{(1)} \tag{B26}$$

and since $K=U_\theta^{(2)}/B_\theta^{(0)}$

$$<BU_{\parallel}>=(1+2q^2)B_\theta^{(0)}U_\theta^{(2)}+B_\varphi^{(0)}U_\varphi^{(1)}$$

$$<BU_{\parallel}>=\frac{1}{J^{(0)}}\left[(1+2q^2)rU_\theta^{(2)}+qRU_\varphi^{(1)}\right] \tag{B27}$$

where $J^{(0)}=r/B_\theta^{(0)}$ is the zero order Jacobian in the standard geometry . The Jacobian J can be written as:

$$J=h_r h_\theta h_\varphi=\frac{h_\theta}{B_\theta}=\frac{r}{B_\theta}=\frac{r}{B_\theta^{(0)}}\left(1+\frac{r}{R_0}\cos\theta\right)=J^{(0)}\left(1+\frac{r}{R_0}\cos\theta\right) \tag{B28}$$

And it can be integrated over the poloidal angle

$$\oint J\,d\theta=J^{(0)}\oint\left(1+\frac{r}{R_0}\cos\theta\right)d\theta=2\pi J^{(0)} \tag{B29}$$

This factor is not important because it will arise in front of every term when averaging the parallel momentum equation cancelling each other.

$$<BU_{\parallel}>=\frac{\oint JBU_{\parallel}\,d\theta}{\oint J\,d\theta}=\frac{1}{2\pi J^{(0)}}\oint JBU_{\parallel}\,d\theta \tag{B30}$$

Combining (B27) and (B30) we find

$$\oint\frac{d\theta}{2\pi}JBU_{\parallel}=(1+2q^2)rU_\theta^{(2)}+qRU_\varphi^{(1)} \tag{B31}$$

And the time derivative of (B31) will be

$$\oint \frac{d\theta}{2\pi} J B \frac{\partial U_{\parallel}}{\partial t} = (1+2q^2) r \frac{\partial U_{\theta}^{(2)}}{\partial t} + q R \frac{\partial U_{\varphi}^{(1)}}{\partial t} \tag{B32}$$

The second term in the right hand side of (B32) is the first term in the r.h.s of the equation (9") in Ref. [8]. This term and the $\eta_{2,i}$ term in equation (19c) in Ref. [8] will eliminate each other in view of the ambipolarity equation [8].

Appendix C. Time scales for ALCATOR C-MOD

The time scale of a differential equation having a first order in time is calculated as the ratio of the linear term to the time derivative term. Here, the toroidal time scale will be calculated from the toroidal momentum equation and the poloidal time scale from the parallel momentum equation.

Time scale of the toroidal momentum equation:

$$m_i N_{isep} \frac{B_{\theta sep}}{B_\varphi} \frac{c_{isep}}{\tau_T} = \frac{B_{\theta sep}}{B_\varphi} \frac{\eta_{2sep} c_{isep}}{L_\psi^2} \quad \text{(C1)}$$

$$\tau_T = 0.833 \frac{m_i L_\psi^2 \Omega_i^2}{T_{sep}} \tau_{isep} \quad \text{(C2)}$$

Time scale of the poloidal momentum equation:

$$m_i N_{sep} (1+2q^2) \frac{B_{\theta sep}^2}{B_\varphi^2} \frac{c_{isep}}{\tau_P} = \frac{3}{2} \frac{B_{\theta sep}^2}{B_\varphi^2} \frac{\eta_{0sep} c_{isep}}{R^2} \quad \text{(C3)}$$

$$\tau_P = 0.694 \frac{m_i R^2 (1+2q^2)}{T_{sep} \tau_{isep}} \quad \text{(C4)}$$

And the ratio of the two time scale is found as:

$$\frac{\tau_T}{\tau_P} = 1.2 \frac{L_\psi^2}{R^2} \frac{\Omega_i^2 \tau_{isep}^2}{(1+2q^2)} \quad \text{(C5)}$$

The inflexion point values for the ALCATOR C-MOD are [30, 31]:

T_{sep}=45 eV, $N_{e,sep}$=$N_{i,sep}$=7×10^{19} m^{-3}, L_ψ=7.6×10^{-3} m, r_{sep}=0.215 m, Z=1.57, R=0.67 m, B_θ=0.625 T, B_φ=5.2 T, B=5.24 T

Safety factor:

$$q_{sep} = \frac{r_{sep} B_\varphi}{R B_\theta} = \frac{0.215\times5.2}{0.67\times0.625} = 2.67 \quad \text{(C6)}$$

Larmor Frequency:

$$\Omega_{isep} = \frac{e_i B}{m_i} = \frac{1.6022\times10^{-19}\times5.24}{1.6726\times10^{-27}} = 5.02\times10^8 \, s^{-1} \quad \text{(C7)}$$

Coulomb Logarithm [32]

$$\ln\Lambda = 17.3 - \frac{1}{2}\ln\left(\frac{N_e}{10^{20}}\right) + \frac{3}{2}\ln T_i, \ \text{T in keV} \quad \text{(C8)}$$

$$\ln\Lambda_{sep} = 17.3 - \frac{1}{2}\ln\left(\frac{7\times10^{19}}{10^{20}}\right) + \frac{3}{2}\ln 0.045 = 12.83 \quad \text{(C9)}$$

Ion collision time [32]

$$\tau_{isep} = 6.6\times10^{17}\left(\frac{m_i}{m_p}\right)^{1/2}\frac{T_{isep}^{3/2}}{N_{isep}\ln\Lambda},\ \text{T in keV},\ \frac{m_i}{m_p} = 1.57 \tag{C10}$$

$$\tau_{isep} = 6.6\times10^{17}\times1.57^{1/2}\times\frac{(0.045)^{3/2}}{7\times10^{19}\times12.83} = 8.79\times10^{-6}\ \text{s} \tag{C11}$$

The toroidal time scale:

$$\tau_T = 0.833\frac{m_i L_\psi^2 \Omega_{sep}^2}{T_{sep}}\tau_{isep} \tag{C12}$$

$$\tau_T = 0.833\frac{1.6726\times10^{-27}\times(7.6\times10^{-3})^2\times(5.02\times10^{8})^2}{45\times1.6022\times10^{-19}}8.79\times10^{-6} = 0.024\ \text{s} \tag{C13}$$

The poloidal time scale:

$$\tau_P = 0.694\frac{m_i R^2(1+2q^2)}{T_{sep}\tau_{isep}} \tag{C14}$$

$$\tau_P = 0.694\times\frac{1.6726\times10^{-27}\times(0.67)^2\times(1+2\times2.67^2)}{45\times1.6022\times10^{-19}\times8.79\times10^{-6}} = 1.25\times10^{-4}\ \text{s} \tag{C15}$$

And the ratio of the two time scale now becomes:

$$\frac{\tau_T}{\tau_P} = \frac{0.024}{1.25\times10^{-4}} = 192 \tag{C16}$$

Acknowledgement

This work was supported in part by the cooperation agreement between the Scientific and Technical Research Council of Turkey (TÜBITAK) and the Forschungszentrum Jülich.

References

[1] Stringer, T.E., Phys. Rev. Letters, **22**, 770 (1969).

[2] Rosenbluth, M.N., Taylor, J.B., Phys. Rev. Letters, **23**, 367 (1969).

[3] Hassam, A.B., Antonsen, Jr., T.M., Phys. Plasmas, **1**, (2), 337 (1994).

[4] Rogister, A.L., J.E. Rice, A. Nicolai, A. Ince-Cushman, S. Gangadhara and Alcator C-Mod Group, Nucl. Fusion, **42** (9), 1144 (2002).

[5] Coppi, B., Nucl. Fusion, **42** (1), 1 (2002).

[6] Rogister, A., Phys. Plasmas, **1** (3), 619 (1994).

[7] Claassen, H.A., Gerhauser, H., Czech. J. Phys. **49**, Suppl. S3, 69 (1999).

[8] Claassen, H.A., et. al., Phys. Plasmas, **7** (9) 3699 (2000).

[9] Mikhailowsky, A.B., Tsypin, V.S., Beitr. Plasmaphys. **24**, 335 (1984).

[10] Hirshman, S. P., Nucl. Fusion, **18**, 7, 917 (1978).

[11] Rosenbluth, M.N., Hinton, F.L., Nucl. Fusion, **36**, 1, 55 (1996).

[12] Daybelge, U., Yarim, C., Anguelova, M., Proceedings of the 7th European Fusion Theory Conference, Jülich, Germany (1997).

[13] Kevorkian, J. and Cole, J. D., Multiple Scale and Singular Perturbation Methods, Springer, New York (1996).

[14] Nicolai, A., Rogister, A., Daybelge, U., Contrib. Plasma Phys. **42**, 241 (2002).

[15] Rogister, A., Phys. Plasmas, **6**, 200 (1999).

[16] Tokar, M. Z., Jaspers, R., Koslowski, H. R., et. al., Plasma Phys. Cont. Fusion, **41**, B317 (1999).

[17] Jaspers, R., Private Communication, (2002).

[18] Rice, J. E., Goetz, J., A., Granetz, M. J., Greenwald, M. J., Hubbard, A. E., et. al., Phys. Plasmas, **7,** 1825 (2000).

[19] Lazzaro, E., Buttery, R. J., Hender, T., Zanca, P., et al., Phys. of Plasmas, 9, 3906 (2002)

[20] Bigi, M., Private Communication (2002).

[21] Shaing, K. C., Hirshman, S. P., Callen, J. D., Phys. Fluids 29, (2), 521 (1986).

[22] Coronado, M., Wobig, H., Phys. Fluids, 29, 527 (1988).

[23] Field Line and Orbit Code for the Study of Ripple Beam Injection into Tokamaks, Report OLRNL/TM-6293.

[24] Nicolai, A., et al., to be published.

[25] Hazeltine, R. D., Phys. Fluids, 17, 961 (1974).

[26] Rogister, A. L., Physical Review Letters, 81, 3663 (1998).

[27] Hazeltine, R. D., Meiss, J. D., Plasma Confinement, Addison-Wesley, California (1992).

28] Rogister, A., Private Communication (1999).

[29] Rogister, A., Li, D., Physics of Fluids B, 4, 804 (1992).

[30] Nicolai, A., Daybelge, U., Rogister, A., Yarim, C., Technical Report Jül-3958, Forschungszentrum Jülich (2002).

[31] Rice. J. E., *et al*, Phys. Plasmas **7**, 1825 (2000).

[32] Wesson, J., Tokamaks, Clarendon Press, Oxford (1997).

Forschungszentrum Jülich
in der Helmholtz-Gemeinschaft

Jül-4091
Oktober 2003
ISSN 0944-2952